



Global changes in  
dryland vegetation  
dynamics

N. Andela et al.

This discussion paper is/has been under review for the journal Biogeosciences (BG).  
Please refer to the corresponding final paper in BG if available.

# Global changes in dryland vegetation dynamics (1988–2008) assessed by satellite remote sensing: combining a new passive microwave vegetation density record with reflective greenness data

N. Andela<sup>1</sup>, Y. Y. Liu<sup>2,4</sup>, A. I. J. M. van Dijk<sup>3,4</sup>, R. A. M. de Jeu<sup>1</sup>, and T. R. McVicar<sup>4</sup>

<sup>1</sup>Earth and Climate Cluster, Department of Earth Sciences, Faculty of Earth and Life Sciences, VU-University, Amsterdam, the Netherlands

<sup>2</sup>Water Research Centre, School of Civil and Environmental Engineering, University of New South Wales, Sydney, Australia

<sup>3</sup>Fenner School of Environment & Society, The Australian National University, Canberra, Australia

<sup>4</sup>CSIRO Land and Water, GPO Box 1666, Canberra, 2601, ACT, Australia

Received: 12 April 2013 – Accepted: 9 May 2013 – Published: 28 May 2013

Correspondence to: N. Andela (n.andela@vu.nl)

Published by Copernicus Publications on behalf of the European Geosciences Union.

Title Page

Abstract

Introduction

Conclusions

References

Tables

Figures



Back

Close

Full Screen / Esc

Printer-friendly Version

Interactive Discussion



## Abstract

Drylands, covering nearly 30 % of the global land surface, are characterized by high climate variability and sensitivity to land management. Here, two satellite observed vegetation products were used to study the long-term (1988–2008) vegetation changes of global drylands: the widely used reflective-based Normalized Difference Vegetation Index (NDVI) and the recently developed passive-microwave-based Vegetation Optical Depth (VOD). The NDVI is sensitive to the chlorophyll concentrations in the canopy and the canopy cover fraction, while the VOD is sensitive to vegetation water content of both leafy and woody components. Therefore it can be expected that using both products helps to better characterize vegetation dynamics, particularly over regions with mixed herbaceous and woody vegetation. Linear regression analysis was performed between antecedent precipitation and observed NDVI and VOD independently to distinguish the contribution of climatic and non-climatic drivers in vegetation variations. Where possible, the contributions of fire, grazing, agriculture and CO<sub>2</sub> level to vegetation trends were assessed. The results suggest that NDVI is more sensitive to fluctuations in herbaceous vegetation, which primarily use shallow soil water whereas VOD is more sensitive to woody vegetation, which additionally can exploit deeper water stores. Globally, evidence is found for woody encroachment over drylands. In the arid drylands, woody encroachment seems to be at the expense of herbaceous vegetation and a global driver is interpreted. Trends in semi-arid drylands vary widely between regions, suggesting that local rather than global drivers caused most of the vegetation response. In savannas, besides precipitation, fire regime plays an important role in shaping trends. Our results demonstrate that NDVI and VOD provide complementary information, bringing new insights on vegetation dynamics.

BGD

10, 8749–8797, 2013

## Global changes in dryland vegetation dynamics

N. Andela et al.

Title Page

Abstract

Introduction

Conclusions

References

Tables

Figures



Back

Close

Full Screen / Esc

Printer-friendly Version

Interactive Discussion



## 1 Introduction

Drylands cover nearly 30 % of the global land surface, they are characterized by high climate variability and are sensitive to land use practice (Tietjen et al., 2010). Over the last decades, many dryland ecosystems have faced increased pressure from human demands and climate change (Asner et al., 2004; Dore, 2005; Liu et al., 2013a). Here we define *arid drylands* as all areas that have a ratio of long-term mean annual precipitation to mean annual potential evaporation of  $0.1 < P/ET_p \leq 0.3$  and *semi-arid drylands* as  $0.3 < P/ET_p \leq 0.7$ . Globally the primary drivers of vegetation dynamics in drylands include: (i) climate (Herrmann et al., 2005; Bai et al., 2008); (ii) fire regime (Bond and Keeley, 2005; Archibald et al., 2010); (iii) grazing (Asner et al., 2004; Liu et al., 2013b); (iv) agriculture (Piao et al., 2003; Jeyaseelan et al., 2007); and (v) atmospheric CO<sub>2</sub> concentrations (Bond and Midgley, 2012; Donohue et al., 2013). Of these, fire, grazing and agriculture can be considered the main land cover related processes that affect large scale vegetation trends in drylands. Other factors, e.g., nitrogen deposition and changes in growing season length (Bai et al., 2008) may also play an important role locally. Changes in the five primary drivers are expected to result in differential responses of woody cover (i.e., woody encroachment or decline) and herbaceous cover (Archer et al., 1995; Van Auken, 2000; Bond et al., 2003; Asner et al., 2004).

Although supporting evidence has been found that each of the five primary drivers can result in responses of dryland vegetation cover, simultaneous changes of the five primary drivers and interactions among them and interaction with ecosystem processes make it difficult to attribute change to any single driver (Bond and Midgley, 2012). Using remote sensing data the evidence of climate impacting vegetation dynamics has been studied at regional (Evans and Geerken, 2004; Herrmann et al., 2005; Wessels et al., 2007), continental (Donohue et al., 2009) and global scales (Nemani et al., 2003). To date, the impact of grazing and fire have not been included in global studies of dryland vegetation dynamics (e.g., Nemani et al., 2003; Fensholt et al., 2012; de Jong et al., 2011). Remote sensing data on global fire regimes are available, with many improved

BGD

10, 8749–8797, 2013

### Global changes in dryland vegetation dynamics

N. Andela et al.

Title Page

Abstract

Introduction

Conclusions

References

Tables

Figures



Back

Close

Full Screen / Esc

Printer-friendly Version

Interactive Discussion



## Global changes in dryland vegetation dynamics

N. Andela et al.

Title Page

Abstract

Introduction

Conclusions

References

Tables

Figures



Back

Close

Full Screen / Esc

Printer-friendly Version

Interactive Discussion



products becoming available since the launch of MODIS in 1999 (Kaufman et al., 1998). Studies of fire induced vegetation change are mainly performed regionally (e.g., Flannigan et al., 2009; Archibald et al., 2010; Heisler et al., 2003) with notable exceptions focusing on longer time scales (Bowman et al., 2009; Bond et al., 2005). Vegetation indices have been widely used as indicators for advances in agricultural practice (e.g., irrigation and fertilization) and annual crop yields (e.g., Tottrup and Rasmussen, 2004), while land cover maps provide information on the spatial extend of agriculture. Several studies provide field evidence of the impact of grazing (Van Auken, 2000; Asner et al., 2003) and rising CO<sub>2</sub> levels (McMahon et al., 2010; Buitenwerf et al., 2011) on vegetation cover; however, these studies are regional, presumably to avoid problems of complexity and data availability. As a consequence, at a global scale the relative importance of climate, fire, grazing, agriculture and CO<sub>2</sub> on vegetation dynamics is still actively debated and so far unresolved (Archer et al., 1995; Asner et al., 2004; Bond and Keeley, 2005; Bond et al., 2005; Fensham et al., 2005; Sankaran et al., 2005; Buitenwerf et al., 2011; Lehmann et al., 2011; Bond and Midgley, 2012).

Satellite remote sensing is a powerful tool to globally study both woody encroachment and desertification, complementing local to regional field evidence and process studies. The Normalized Difference Vegetation Index (NDVI) is the most widely used spectral vegetation index and is based on a ratio of red and near infrared reflectance (Rouse et al., 1974; Tucker, 1979; Beck et al., 2011). NDVI has been used as an indicator of vegetation productivity (Tucker et al., 1985; McVicar and Jupp, 1998); and is related to Leaf Area Index (LAI; Wang et al., 2005), canopy cover fraction and the fraction of absorbed photosynthetically active radiation (fPAR; Asrar et al., 1984; Carlson and Ripley, 1997; Lu et al., 2003). Complementary to the NDVI, a recently developed dataset is Vegetation Optical Depth (VOD). VOD describes the transparency of vegetation in the microwave domain and is mostly sensitive to vegetation water content (Kirdiashev et al., 1979). Owe et al. (2001) developed the Land Parameter Retrieval Model (LPRM) to derive VOD from low frequency passive microwave observations. This model was further improved by Meesters et al. (2005) and has been applied to a

series of passive microwave sensors (Owe et al., 2008). VOD is sensitive to vegetation water content in both the woody and leafy vegetation components, and provides a measure of above-ground biomass (Liu et al., 2011a).

Separately, both reflective and microwave products have been used to study vegetation dynamics. Pettorelli et al. (2005) reviews ecological studies that used NDVI to examine climate- and human-induced vegetation change (e.g., Evans and Geerken, 2004; Herrmann et al., 2005; Wessels et al., 2007), global vegetation trends (e.g., de Jong et al., 2011; Fensholt et al., 2012) and land degradation (e.g., Bai et al., 2008). Long VOD time series were only recently developed, and have been used to study vegetation phenology (Jones et al., 2011, 2012) and to show the impact of El Niño Southern Oscillation on Australian vegetation cover (Liu et al., 2007). Global trends in VOD were shown to correspond to changes in precipitation, livestock (e.g., overgrazing), crop production, deforestation and fires (Liu et al., 2013a,b).

To date, only introductory assessment of NDVI and VOD co-trends has been performed (Liu et al., 2011a). While many regions had similar co-trends regional differences were illustrating that VOD provides new information for mixed woody-herbaceous land cover types. Detailed analysis of the driver-response relationships of the complementary NDVI and VOD responses was not conducted (Liu et al., 2011a). Due to the characteristics of both products, differential responses in mixed woody-herbaceous land cover types are expected (Shi et al., 2008). Compared to VOD, NDVI saturates at relatively low biomass and is therefore most sensitive to vegetation covering the largest surface (Tucker, 1979). As a consequence, temporal correlation between NDVI and VOD is high for grass and crop-lands but lower for high biomass vegetation types where NDVI saturates (Liu et al., 2011a). Grasses are the main source of large interannual variation in NDVI for savanna ecosystems (Archibald and Scholes, 2007; Roderick et al., 1999b; Lu et al., 2003; Donohue et al., 2009). VOD has a greater penetration capacity and is more sensitive to changes in woody vegetation (Liu et al., 2011a; Shi et al., 2008). The relationship between NDVI and VOD is further explored in the background theory section.

## Global changes in dryland vegetation dynamics

N. Andela et al.

Title Page

Abstract

Introduction

Conclusions

References

Tables

Figures



Back

Close

Full Screen / Esc

Printer-friendly Version

Interactive Discussion



This paper uses the two complementary remote sensing datasets and analyzes their trends across the global drylands. In particular, we address the following questions:

1. How do NDVI and VOD complement each other and what do combined trends tell us about vegetation dynamics?
2. What component of temporal dryland vegetation dynamics is explained by precipitation?
3. What are the remaining trends in both vegetation indices, and how are they related to the other primary drivers (fire, grazing, agriculture and CO<sub>2</sub>)?

Differences between NDVI and VOD are explored and trends are interpreted ecologically. A model is developed to predict the vegetation responses that can be accounted for by precipitation variation. Residual trends (i.e., the observed minus model-explained trends) and their potential drivers are discussed and attributed, where possible, using global data on burned area, grazing and literature. The results elucidate changes in global dryland biomass and composition, and provide a spatially explicit analysis across the global drylands of previously primarily locally applied conceptual frameworks. Despite the limited data availability on the drivers associated with land use; we find that information on regional ecosystems (e.g., land cover type and water availability) in combination with knowledge of grazing intensity and burned area time series can provide important information on trends in vegetation density and composition.

## 2 Background theory

A conceptual framework is required to relate temporal patterns and trends in NDVI and VOD to vegetation characteristics. For NDVI, the reflectance observations from which it is derived can be thought of as a linear mixture of the constituent surface reflectance components:

$$\rho = f_o \rho_o + (1 - f_o)(f_u \rho_u + f_s \rho_s) \quad (1)$$

## Global changes in dryland vegetation dynamics

N. Andela et al.

Title Page

Abstract

Introduction

Conclusions

References

Tables

Figures



Back

Close

Full Screen / Esc

Printer-friendly Version

Interactive Discussion



## Global changes in dryland vegetation dynamics

N. Andela et al.

Title Page

Abstract

Introduction

Conclusions

References

Tables

Figures



Back

Close

Full Screen / Esc

Printer-friendly Version

Interactive Discussion



where  $\rho$  is the wavelength reflectance and  $f$  the fraction canopy cover with subscripts denote overstory ( $o$ ), understory ( $u$ ) and soil surface ( $s$ ). Homogeneous vegetation cover is assumed such that the overstory will obscure some part of the understory, and it is assumed that the NDVI observations are representative for nadir measurements such that  $f$  equates to projected canopy cover. Here it is assumed that the overstory and understory can be assumed equal to the (woody) persistent and (herbaceous) recurrent vegetation components (cf. Roderick et al., 1999b; Lu et al., 2003; Donohue et al., 2009). NDVI is calculated as a reflectance difference index and therefore, using Eq. (1) it can be shown that NDVI will respond to surface component mixing ratios in a slightly non-linear manner, although NDVI still converges to end member NDVI values when these dominate overall reflectance (Asner, 1998). NDVI per unit canopy area for recurrent vegetation tends to exceed that of persistent vegetation. Because the NDVI is responsive to leaf chlorophyll concentration, this may be interpreted as a result of functional convergence between leaf chlorophyll, structural properties, leaf life span and life form, with recurrent vegetation having shorter-lived and 'greener' leaves (Reich et al., 1997, 2003). As a result, all else being equal, an increase in NDVI can be explained by an increase in total canopy cover or a relative increase in recurrent vegetation canopy cover, or both.

VOD (denoted  $\tau$ ) can be interpreted as being linearly related to total above-ground biomass (AGB) water content, i.e., the sum of water in woody and non-woody vegetation (Jackson et al., 1982; Wigneron et al., 1993):

$$\tau = \tau_o + \tau_u = c_\tau(\theta_o m_o + \theta_u m_u) \quad (2)$$

where  $\theta$  is vegetation water content,  $m$  the AGB, and  $c_\tau$  the constant of proportionality.  $\theta$  will normally be greater for herbaceous vegetation than for woody vegetation (Roderick et al., 1999a, 2000), therefore increases in VOD can mean an increase in total AGB, an increase of the fraction of herbaceous vegetation AGB, or both.

Finally, the relationship between NDVI and VOD is influenced by the connection between AGB ( $m$ ) and canopy cover ( $f$ ). This relationship can be presented by considering

the commonly used light extinction equation (Monsi and Saeki, 2005) that relates  $f$  to leaf area index ( $\Lambda$ ):

$$f = 1 - \exp(-\kappa\Lambda) = 1 - \exp(-\kappa\alpha_{\text{SLA}}f_{\text{leaf}}m) = 1 - \exp(-c_{\Lambda}m) \quad (3)$$

where  $\kappa$  is the extinction coefficient,  $\alpha_{\text{SLA}}$  the specific leaf area (i.e., area per unit leaf mass), and  $f_{\text{leaf}}$  the fraction of leaf biomass in total AGB. While  $\kappa$  depends on leaf orientation and clumping,  $f_{\text{leaf}}$  and  $\alpha_{\text{SLA}}$  will be greater for non-woody vegetation than for woody vegetation. Overall, total AGB remaining unchanged, the sensitivity of NDVI to a relative increase in the herbaceous component is expected to be considerably greater than the sensitivity of VOD. VOD, being sensitive to AGB water content, is expected to be more sensitive to a relative increase in woody vegetation. Per unit mass the tree foliage will have a somewhat higher relative water content than the woody parts, but because woody biomass typically represents 90% or more of total above-ground biomass (Northup et al., 2005, and references therein) and it still contains most of the water (Sternberg and Shoshany, 2001). The above considerations lead to the following four expectations:

1. an increase in both NDVI and VOD signifies an increase in the herbaceous biomass component and/or an increase in total AGB;
2. an increase in NDVI combined with a decrease in VOD signifies an increase in the herbaceous component;
3. a decrease in NDVI and an increase in VOD signifies an increase in the woody component; and
4. a decrease in both NDVI and VOD signifies a decrease in the herbaceous biomass component and/or a decrease in total AGB.

## BGD

10, 8749–8797, 2013

### Global changes in dryland vegetation dynamics

N. Andela et al.

Title Page

Abstract

Introduction

Conclusions

References

Tables

Figures



Back

Close

Full Screen / Esc

Printer-friendly Version

Interactive Discussion



### 3 Materials

To study global long-term dryland vegetation dynamics, both NDVI and VOD datasets were used for their overlapping period 1988–2008. Both vegetation indices are dimensionless and here we use a 0.25° spatial and monthly temporal resolution.

#### 3.1 Normalized Difference Vegetation Index (NDVI)

The NDVI data are Global Inventory Modeling and Mapping Studies 3rd generation (GIMMS3g) derived from the Advanced Very High Resolution Radiometer (AVHRR) sensor on board the NOAA series of satellites (i.e., NOAA 7, 9, 11, 14, 16 and 17; Tucker et al., 2005). The data were resampled from 1/12° to 0.25° spatial resolution and from twice to once monthly temporal resolution by simple averaging. Data were available between 1981–2010. Recently Beck et al. (2011) showed that of four AVHRR processing chains tested, GIMMS was best able to track trends in 1424 Landsat image pairs. Sensor characteristics and atmospheric variations introduce uncertainty in the NDVI signal over non-vegetated surfaces, including snow and ice (Brown et al., 2006).

#### 3.2 Vegetation Optical Depth (VOD)

Liu et al. (2011a) developed a harmonized VOD dataset for 1988–2008 by merging VOD retrievals from SSM/I (Special Sensor Microwave Imager, 1988–2007), TMI (the microwave instrument onboard the Tropical Rainfall Measuring Mission satellite, 1998–2008) and AMSR-E (the Advanced Microwave Scanning Radiometer – Earth Observing System, July 2002–2008) using the LPRM algorithm. This harmonized dataset preserves the relative dynamics (e.g., seasonality and interannual variations) of the original products (Liu et al., 2011b) and is able to capture long-term changes in total aboveground vegetation water content and biomass over various land cover types globally (Liu et al., 2013a). The VOD data should be interpreted with caution over sandy

BGD

10, 8749–8797, 2013

## Global changes in dryland vegetation dynamics

N. Andela et al.

Title Page

Abstract

Introduction

Conclusions

References

Tables

Figures

⏪

⏩

◀

▶

Back

Close

Full Screen / Esc

Printer-friendly Version

Interactive Discussion



deserts, open water and under the frost conditions (de Jeu, 2003; Jones et al., 2011; Gouweleeuw et al., 2012).

### 3.3 Additional datasets

#### 3.3.1 Precipitation

5 Precipitation data (monthly; 1901–2009) produced by the University of East Anglia Climatic Research Unit (CRU Time Series version 3.1) were available at a 0.5° resolution (Jones and Harris, 2008). For analysis it was assumed that within this grid cell precipitation was homogeneously distributed and data was resampled to a 0.25° resolution.

#### 3.3.2 Land cover

10 The MODIS Land Cover Type Yearly Climate Modeling Grid (MCD12C1; 2005; 0.05° resolution), land cover map was used here (NASA, 2008). Data was resampled to a 0.25° resolution using the land cover with the highest frequency in each grid cell. The land cover types follow the University of Maryland (UMD) classification scheme (Hansen et al., 2000). For our analysis some land cover classes were merged to assist  
15 interpretation (i.e., urban and built-up, barren or sparsely vegetated, and unclassified + fill were here merged into “barren or sparsely vegetated”; all types of forest into “forest”; and closed and open shrublands into “shrublands”).

#### 3.3.3 Fire

20 Monthly burned area data was available based on MODIS Terra satellite imagery MCD-64A1; 500 m resolution; November 2000 onwards (Giglio et al., 2009). Data was rescaled to a monthly 0.25° resolution by calculating the mean burned area per 0.25° grid cell.

## Global changes in dryland vegetation dynamics

N. Andela et al.

Title Page

Abstract

Introduction

Conclusions

References

Tables

Figures



Back

Close

Full Screen / Esc

Printer-friendly Version

Interactive Discussion



### 3.3.4 Livestock

Livestock density was available from the Food and Agriculture Organization's (FAO) Gridded Livestock of the World data ([http://www.fao.org/AG/againfo/resources/en/glw/GLW\\_dens.html](http://www.fao.org/AG/againfo/resources/en/glw/GLW_dens.html); Robinson et al., 2007) and was expressed in Tropical Livestock Units (TLU) per km<sup>2</sup> (1 TLU = 250 kg live weight, cattle = 0.7 TLU, sheep and goats = 0.1 TLU; Jahnke, 1982). The FAO livestock density data has a spatial resolution of 0.05° and is not temporally varying hence time series analysis of this driver could not be performed.

## 4 Methods

### 4.1 Relationship between NDVI and VOD

To illustrate the theoretical relations between NDVI and VOD (Sect. 2), we calculated global mean values and standard deviation for both vegetation indices. To provide more insight, we calculated monthly mean values of NDVI and VOD and compared seasonal patterns of three southern African land cover types with increasing woody cover: (i) grasslands, (ii) savannas and (iii) woody savannas. Next to the global maps of mean values, annual mean values and range (maximum minus minimum) were also calculated and compared for the three previously mentioned land cover types with increasing woody cover. In addition to earlier explorations on the relationship between NDVI and VOD (Liu et al., 2011a; Shi et al., 2008), the results of these analysis were used to verify the four expectations of Sect. 2, regarding the co-trends between NDVI and VOD. Trends in NDVI and VOD were analyzed separately (Sects. 4.2 and 4.3), but co-trends (NDVI and VOD) were also interpreted using our theoretical framework.

**BGD**

10, 8749–8797, 2013

## Global changes in dryland vegetation dynamics

N. Andela et al.

Title Page

Abstract

Introduction

Conclusions

References

Tables

Figures

⏪

⏩

◀

▶

Back

Close

Full Screen / Esc

Printer-friendly Version

Interactive Discussion



## 4.2 Response of vegetation index anomalies to antecedent precipitation anomalies

Following Evans and Geerken (2004) and Herrmann et al. (2005), linear regression models between antecedent precipitation and each vegetation index were developed for each grid cell. These regression models were used to estimate the long-term vegetation trends expected due to precipitation patterns alone. Expected vegetation trends were calculated in three steps. Firstly, anomalies were calculated both for precipitation and the vegetation products (NDVI and VOD). Second, the antecedent precipitation index (API) was calculated, here defined as the optimal correlating precipitation running mean (PRM) as judged from Spearman's ranked correlation coefficient ( $R_s$ ) over 1 to 60 month averaging periods. The  $API(x, y, t)$  was calculated for each grid cell  $(x, y)$  and month  $t$  using:

$$API(x, y, t) = \frac{\sum_{t-(T(x,y)-1)}^t d'(x, y, t)}{T(x, y)}. \quad (4)$$

Where  $T$  is the averaging period in months for antecedent precipitation that leads to the highest  $R_s$  between the PRM and the vegetation anomalies and  $d'$  is the precipitation anomaly. The expected vegetation variation was calculated using as a linear function of API:

$$\text{expected}(x, y, t) = a_1(x, y) \cdot API(x, y, t) + a_2(x, y). \quad (5)$$

For each grid cell the coefficients  $a_1$  and  $a_2$  were determined by least squared differences between the API and vegetation anomaly time series. Similar approaches were used by Evans and Geerken (2004), Herrmann et al. (2005) and Wessels et al. (2007) for NDVI, who also assumed (as we do) that if expected vegetation variation based on precipitation variation was removed from observed vegetation anomalies, the residual trends are largely independent of precipitation. Here we develop models based on

**BGD**

10, 8749–8797, 2013

### Global changes in dryland vegetation dynamics

N. Andela et al.

Title Page

Abstract

Introduction

Conclusions

References

Tables

Figures

◀

▶

◀

▶

Back

Close

Full Screen / Esc

Printer-friendly Version

Interactive Discussion



precipitation and vegetation anomalies (rather than the original vegetation indices) as all trends are present in the anomalies, and not in the seasonal pattern. So a model optimized for anomalies will give a better estimation of trends in the vegetation indices caused by precipitation. Although direct correlation between precipitation and vegetation indices will be higher than correlation between vegetation index and precipitation anomalies, a model based on the original vegetation indices and precipitation would be more suitable to study the effect of precipitation on seasonal rather than interannual vegetation dynamics. However, to facilitate comparison with previous studies, the analysis was also repeated using the original vegetation indices rather than anomalies (cf. Herrmann et al., 2005).

### 4.3 Global dryland vegetation trends

After calculating the expected index anomalies, trends were calculated for the observed, expected and residual vegetation index. The residual trend was calculated as the trend in the observed minus expected vegetation anomaly and represents the component of the signal that could not be directly attributed to precipitation variations. A conventional non-parametric Mann-Kendall trend test was used to determine areas of significant monotonic trends (cf. de Jong et al., 2011; Fensholt et al., 2012; Liu et al., 2013a). The non-parametric Theil-Sen estimator of slope is insensitive to outliers and was used to calculate linear trends (Sen, 1968; Theil, 1950).

Climate and land cover affect NDVI and VOD dynamics and will likely cause them to respond differently to the primary drivers of dryland vegetation dynamics. Hence, to stratify our results, we used global maps of land cover (Fig. 1a) and P/ET<sub>p</sub> classes; referred to as humidity classes hereafter (Fig. 1b). Global maps of livestock density, burned area, recent trends in burned area, and ecosystem characteristics of land cover and humidity were used to interpret results. It was assumed that globally consistent trends not explained by climate, fire, grazing and agricultural developments are caused by increasing atmospheric CO<sub>2</sub> concentrations (Bond et al., 2003; Donohue et al., 2013). Impact of fire on vegetation indices was further explored studying time series of

**BGD**

10, 8749–8797, 2013

## Global changes in dryland vegetation dynamics

N. Andela et al.

Title Page

Abstract

Introduction

Conclusions

References

Tables

Figures

◀

▶

◀

▶

Back

Close

Full Screen / Esc

Printer-friendly Version

Interactive Discussion



NDVI, VOD and burned area for grassland, savanna and woody savanna in southern Africa.

Grid cells with less than 40 % valid data (i.e., 100 or less of the 252-month series) in either vegetation dataset were not included in this analysis. NDVI cannot be used over snow and ice (Brown et al., 2006), while VOD is sensitive to frost conditions (see Sect. 3.2; Liu et al., 2011a), hence seasonally recurrent data gaps exist in both products during winter. The threshold of 40% valid data was chosen to include most drylands at high latitudes/elevations. Data gaps were ignored in trend calculations yet are considered in their interpretation.

## 5 Results

### 5.1 Relationship between NDVI and VOD

The relation between NDVI and VOD was explored calculating their mean and standard deviation for global drylands (Fig. 2). Globally, for the arid drylands, mean VOD values were generally lower than NDVI, with increasing humidity and biomass VOD increased faster than NDVI. Most notable examples of large differences between NDVI and VOD were forests and agricultural regions of the temperate northern hemisphere drylands. NDVI generally showed higher standard deviations than VOD, especially for drylands that face cold winters. Regional exceptions were observed, with standard deviation of VOD being larger for some savanna regions in northern and southern Africa and Australia. More detail was provided by studying three land cover types of southern Africa (study areas are shown in Fig. 3d). With increasing woody cover (i.e., along the gradient from grassland in the south through savanna to woody savanna in the north), VOD increased faster than NDVI (Fig. 3a, b and c). The annual average VOD for grassland was 0.41 and for woody savanna this increased to 0.70 (i.e., a 0.29 increase). In contrast, the annual average NDVI only increased 0.19 (i.e., from 0.43 for grassland to 0.62

**BGD**

10, 8749–8797, 2013

## Global changes in dryland vegetation dynamics

N. Andela et al.

Title Page

Abstract

Introduction

Conclusions

References

Tables

Figures

⏪

⏩

◀

▶

Back

Close

Full Screen / Esc

Printer-friendly Version

Interactive Discussion



for woody savanna). The NDVI range (annual maximum minus minimum) exceeded the VOD range for all three land cover types (Fig. 3a, b and c).

## 5.2 Response of vegetation index anomalies to antecedent precipitation anomalies

5 The strongest correlation ( $R_s$ ) between vegetation anomalies and antecedent precipitation index (API) were observed over arid drylands ( $0.1 < P/ET_p \leq 0.3$ ; Fig. 4a and c). While NDVI and VOD showed similar spatial patterns, VOD showed higher correlation coefficients, suggesting that VOD reacts stronger to interannual precipitation variability in drylands than NDVI. In regions with low or insignificant correlations between vegetation and API, factors other than precipitation are likely to determine interannual vegetation variability and/or variability was minimal over the study period. While for most land cover classes VOD had larger areas with significant correlations, NDVI was more responsive to changes in croplands (Table 1).

15 Averaging periods (denoted  $T$  in the methods; Fig. 4b and d) are related to the capacity of vegetation to use antecedent precipitation and the lead time of interannual variation in precipitation followed by a vegetation response. NDVI generally has shorter averaging periods than VOD (cf. Fig. 4b with d). To facilitate comparison with other studies, model results based on original vegetation indices and precipitation are shown in the annex material (Fig. A1). In general, observed correlation was higher, and averaging periods were shorter for the model based on original vegetation indices and precipitation (Fig. A1) than when compared to the model based on anomalies used here (Fig. 4, see Sect. 4.2). Figure 5 shows box plots of the data in Fig. 4, stratified by land cover and humidity classes. Both NDVI and VOD showed longest averaging periods for areas dominated by woody vegetation and croplands, shorter periods were observed for grasslands and savannas.

25 Figure 6 shows an example of expected and observed anomalies in NDVI and VOD for two  $5^\circ \times 5^\circ$  regions (Fig. 3d): (i) eastern Australia ( $25\text{--}30^\circ$  S,  $145\text{--}150^\circ$  E); and (ii) southern Africa ( $25\text{--}30^\circ$  S,  $20\text{--}25^\circ$  E). Modeled NDVI is based on shorter averaging

**BGD**

10, 8749–8797, 2013

## Global changes in dryland vegetation dynamics

N. Andela et al.

Title Page

Abstract

Introduction

Conclusions

References

Tables

Figures

◀

▶

◀

▶

Back

Close

Full Screen / Esc

Printer-friendly Version

Interactive Discussion



periods, because the signal showed little interannual variation. VOD, on the other hand, is usually based on longer averaging periods and therefore follows the interannual variation in precipitation, being less sensitive to small intra-annual variability.

### 5.3 Global dryland vegetation trends

5 Figure 7a and b show observed annual trends in NDVI and VOD (1988–2008). Some regions showed similar trends in both datasets: e.g., India, Mongolia, North America, eastern Australia, and northern African savannas. Other areas showed contrasting trends between the datasets: e.g., southern Africa, northern Australia, Argentina and central Asia. While observed trends in NDVI and VOD differ considerably, the expected trends in NDVI and VOD were relatively similar and strong decreasing trends were found in southeastern Australia and Mongolia, while increasing trends were found in most of Africa and northern Australia (Fig. 7c and d). Figure 7e and f show residual trends, calculated as observed anomalies minus expected vegetation anomalies. For the NDVI (Fig. 7e) some trends persisted (e.g., positive trends over most of India and Spain, and negative trends over southern Russia and Kazakhstan). In other cases, if observed and expected trends had the opposite direction (i.e., one is positive and the other negative) this resulted in enhanced residual trends (e.g., Argentina, arid northern Africa, southern Africa and northern Australia in the case of NDVI; compare Fig. 7a, c and e). If observed and expected trends had the same direction this resulted in smaller residual NDVI trends (e.g., Mongolian steppe and semi-arid drylands of northern Africa), or trends tended to zero (e.g., southern India and northern China). Finally, in some regions new NDVI trends emerged (southeastern Australia and south-west Western Australia). Observed and expected trends in VOD generally had the same direction, resulting in smaller residual trends (e.g., northern Australia, Sahel, southern Africa and southern Argentina; compare Fig. 7b, d and f). Although there were also regions with observed trend in VOD, but no trends in expected vegetation anomalies (e.g., east Africa and northern India).

BGD

10, 8749–8797, 2013

## Global changes in dryland vegetation dynamics

N. Andela et al.

Title Page

Abstract

Introduction

Conclusions

References

Tables

Figures

◀

▶

◀

▶

Back

Close

Full Screen / Esc

Printer-friendly Version

Interactive Discussion



## Global changes in dryland vegetation dynamics

N. Andela et al.

Title Page

Abstract

Introduction

Conclusions

References

Tables

Figures



Back

Close

Full Screen / Esc

Printer-friendly Version

Interactive Discussion



Box plots of the distribution of observed, expected and residual trends, stratified by land cover and humidity classes, illustrate that NDVI overall had less distinct trends than VOD (Fig. 8). Median observed trends in NDVI were increasing for savanna and croplands, and decreasing for the other land cover classes (Fig. 8a). For VOD decreasing median observed and residual trends were found in forested drylands, while increasing median trends were found for all other land cover classes (Fig. 8a and c). Over arid drylands the median VOD trend was increasing while NDVI showed mostly decreasing trend, for more humid drylands NDVI and VOD trends were more similar and closer to zero. Savannas and shrublands showed a small increase in expected median NDVI and VOD (Fig. 8b), indicating that part of the change in median vegetation index response is explained by trends in precipitation. There were no particular humidity classes that showed a large change in expected median vegetation response, indicating that median changes in precipitation were close to zero for each humidity class (Fig. 8e). In the residual trends (i.e., observed minus expected) similar but smaller median trends remained, both for NDVI and VOD (Fig. 8c and f).

Vegetation trends (Fig. 7), are expected to be related to trends in precipitation (Fig. 9a) and trends in annual burned area (Fig. 9b). Most global drylands experienced stable or increasing precipitation amounts during 1988-2008; notable exceptions are southeast Australia, the Mongolian steppe and northern China (Fig. 9a). Trends in annual burned area declined for northern Africa and increased in most of southern Africa (Fig. 9b). Southern America showed a mixed pattern of increased and declined trends of annual burned area, while trend of annual burned area over most of Australia has been stable or declined. The relationship between burned area and vegetation indices was further analyzed using three study areas with different land cover in southern Africa (locations are shown in Fig. 3d). For grasslands, annual burned area is relatively low and no obvious relationship between vegetation indices and burned area is present (Fig. 10a). In savannas, both NDVI and VOD are strongly related to interannual variation in burned area (Fig. 10b; compare 2006 and 2008 with the other years). For woody savannas,



The co-relationship of NDVI and VOD trends (Fig. 11) provides new insights in the relative performance of herbaceous and woody vegetation components in global drylands. Woody encroachment into grassland or savannas has been observed across the globe, including Argentina (e.g., Adamoli et al., 1990), Africa (e.g., Vegten, 1984) and Australia (Fensham et al., 2005) and are reviewed by Archer et al. (2001). Although satellite observations of NDVI and VOD confirm our theoretical framework, future validation studies, comparing satellite observations with local to regional field studies, can improve regional interpretation and confidence. Vegetation trends will be discussed in greater detail in Sect. 6.3 for arid and semi-arid drylands separately.

## 6.2 Response of vegetation index anomalies to antecedent precipitation anomalies

As expected, arid drylands showed strongest correlation between the vegetation index anomalies and API (i.e., median  $R_s$  NDVI > 0.3, median  $R_s$  VOD > 0.5; see Fig. 5). Nemani et al. (2003) mapped these areas as being water limited, and for higher latitudes, water and temperature limited. Correlation is less strong than found by some other studies (e.g., Herrmann et al., 2005) or when analyzing the original indices (cf. Fig. A1) because seasonal vegetation – precipitation responses are not included. In semi-arid drylands, like the savannas of Africa and Australia, regions that have a strong seasonal precipitation response do not necessarily show a strong interannual response (compare Fig. 4a and c with Fig. A1). This could be explained by a seasonal abundance of water in which variation in precipitation does not affect vegetation followed by a dry season in which the vegetation is unable to use antecedent precipitation. Optimum precipitation averaging periods differ considerably for NDVI and VOD (Figs. 4 and 5) and are larger when the seasonal cycle is included, rather than the anomalies only (compare Fig. 4 with Fig. A1). The model based on original vegetation indices and precipitation is mostly affected by short-term vegetation – precipitation response; here, we use a model based on anomalies, that is sensitive to the long-term capacity of vegetation to use antecedent precipitation.

Title Page

Abstract

Introduction

Conclusions

References

Tables

Figures



Back

Close

Full Screen / Esc

Printer-friendly Version

Interactive Discussion



## Global changes in dryland vegetation dynamics

N. Andela et al.

Title Page

Abstract

Introduction

Conclusions

References

Tables

Figures



Back

Close

Full Screen / Esc

Printer-friendly Version

Interactive Discussion



Following previous studies (Evans and Geerken, 2004; Herrmann et al., 2005; Nemani et al., 2003; Wessels et al., 2007; Donohue et al., 2009), we also found that not all interannual variation can be explained by precipitation alone. VOD generally shows longer averaging periods than NDVI, this is because they are sensitive to different components of vegetation cover (Fig. 3a, b and c); NDVI is more sensitive to changes in the shallow rooted herbaceous understory (Archibald and Scholes, 2007), and VOD more sensitive to changes in the woody overstory, which can also utilize moisture from deeper soil and groundwater stores (Rossatto et al., 2012; House et al., 2003). The stronger correlations between VOD and API are attributed to the larger interannual variation in the VOD dataset and caused by interannual precipitation variations (Fig. 6). Archibald and Scholes (2007) reported similar findings, and concluded that plants that access deeper water and have carbohydrate reserves may show a phenology that is quite different from surrounding areas with grass cover that depend on shallow soil moisture for their growth. It appears that similar conclusions may be drawn for interannual variation.

Each vegetation index separately shows local patterns with sometimes sharp changes and some regions showed considerably longer averaging periods than others (seen as rapid changes in color within each of Fig. 4b and d). This particularly occurs in areas of weak correlation between API and vegetation indices. However, some regions (e.g., west Australia and southern Africa) show strong correlation and large local differences in averaging periods, this seems to be due to the presence (or absence) of large interannual variation in precipitation. Distinct local patterns suggest that the physical landscape, including landform and soil type, likely contribute.

### 6.3 Global dryland vegetation trends

Vegetation trends of the world's arid drylands and semi-arid drylands are discussed in turn. Overall, the world's drylands show a decrease in NDVI and an increase in VOD (Fig. 8d).

### 6.3.1 Arid drylands ( $0.1 < P/ET_p \leq 0.3$ )

Many arid drylands experienced unchanged or increasing annual precipitation (Fig. 9b), and median expected trends in both vegetation indices were close to zero (Fig. 8e). NDVI median trend for arid drylands was negative while VOD median trend was positive (Fig. 8e). Both the relatively constant or increasing VOD trends and most negative trends in NDVI remain after precipitation induced variation is accounted for (Fig. 7e and f). This results in many regions showing opposite trends in NDVI and VOD (Fig. 11; e.g., arid drylands of Argentina, southern Africa, northern Africa and Australia). In those regions, it seems that woody encroachment takes place at the expense of the herbaceous understory. Woody encroachment has been attributed to climate (Fensham et al., 2005), fire regime (Sankey et al., 2012), grazing (Asner et al., 2004) and CO<sub>2</sub> fertilization (Buitenwerf et al., 2011).

Clear trends in the NDVI and VOD residuals indicate that next to precipitation, other drivers also play a role (Fig. 7e and f). A possible explanation for residual trends could be changing fire regimes (Fig. 9b) through its impact on competitiveness of the herbaceous and woody vegetation components (Sankey et al., 2012). Bowman et al. (2009) showed that annual burned area is highest in areas of intermediate primary production, limited by a lack of dry periods towards the tropics and limited by a lack of fuel towards dry areas (Fig. 9d). Primary production is the main limitation on annual burned area in these drier regions (Archibald et al., 2009). This results in a system of highly variable biomass production, followed by infrequent fires (Fig. 10a). Increasing precipitation is expected to increase annual burned area in arid drylands. Increased burning can impact dry season minimum NDVI values (Fig. 10; Díaz-Delgado et al., 2003) and suppress woody encroachment (Lehmann et al., 2011). However, recent (2000–2011) trends in annual burned area do not show increases in most arid drylands and showed declines in northern Australia and the Sahel (Fig. 9b). This, combined with an average annual burned area of below 10% (Fig. 9d), seems to make fire an unlikely driver of globally observed changes.

## Global changes in dryland vegetation dynamics

N. Andela et al.

Title Page

Abstract

Introduction

Conclusions

References

Tables

Figures



Back

Close

Full Screen / Esc

Printer-friendly Version

Interactive Discussion



Decreasing NDVI trends have been interpreted as a proxy for land degradation (Wes-

sels et al., 2007; Bai et al., 2008) which might be caused by grazing. Grazing has also

been associated with woody encroachment (e.g., Asner et al., 2004). Although grazing

might cause contradicting trends between NDVI and VOD in some regions (e.g., arid

parts of northern Africa) similar trends are observed in regions of limited or no grazing

by domestic livestock (e.g., compare Figs. 9c and 11 for arid drylands of Argentina

and Australia). The spatial patterns and scale at which trends occur suggest that graz-

ing by domestic livestock is not the main driver in these cases, impact of grazing by

non-domesticated animals was not included here, as no information was available.

Sankaran et al. (2005) suggest that woody vegetation receiving less than 350 mm an-

annual precipitation is largely constrained by water availability. Rising atmospheric CO<sub>2</sub>

concentrations affects water use efficiency and photosynthetic rates (Donohue et al.,

2013) as well as light and nutrient efficiency (Drake et al., 1997; Farquhar, 1997).

CO<sub>2</sub> is reported to enhance the relative performance of woody C3 species over the

C4 grasses that dominate tropical savannas (Bond and Midgley, 2012; Higgins and

Scheiter, 2012). Once woody plants are established in savannas, they are likely to limit

the growth of herbaceous plants by water uptake and shading (Breshears, 2006).

Increases in extreme air temperatures and changes in growing season duration can

also explain some of the observed vegetation trends (Allen et al., 2010). Changing

duration of rain seasons can impact the relative performance of different species: a

shorter but more intense wet season is likely to result in decreasing herbaceous un-

derstory (NDVI) during dry seasons, while deep rooted vegetation suffers less, having

access to deeper water resources and therefore being more sensitive to long-term wa-

ter availability (Fig. 5; Archibald and Scholes, 2007). Evidence for shortening growing

seasons is found for arid drylands of northern Africa (de Jong et al., 2011). Tietjen et al.

(2010) argue that grasses lose competitive strength under decreasing soil moisture

resulting in thickening woody vegetation comprised of shrubs. Other possible explana-

tions could be shifts in grass types, both affecting NDVI values directly and changing fire

regimes (Brooks et al., 2004). Finally, increased air temperatures can result in higher

evaporation rates and during the dry season result in a competitive advantage of deep rooted species over shallow rooted species. Although air temperature is increasing over many drylands globally, decreasing trends are also observed in some regions, as temperature tends to be strongly related to precipitation through the effect of cloud cover on solar irradiation. Additionally, decreases in wind speed (“wind stiling”), and changes in other meteorological variables governing the evaporative process, also alter the evaporative regime (McVicar et al., 2012). Following Higgins and Scheiter (2012), we suggest that the effects of changing evaporation rates in drylands are less important than the effects of increasing atmospheric CO<sub>2</sub> concentrations. Given that patterns in the residual trends are found in most global arid drylands, all experiencing very different fire and grazing conditions (compare Fig. 7e and f with Fig. 9c and d), a global driver such as CO<sub>2</sub> fertilization appears more plausible.

### 6.3.2 Semi-arid drylands ( $0.3 < P/ET_p \leq 0.7$ )

The distribution of trends in vegetation indices differs between humidity classes and land cover classes (Fig. 8). The median trend in NDVI is around zero for semi-arid drylands, showing positive trends over savannas and croplands and negative median trends for other land cover classes. VOD shows positive median trends for all land cover classes except forest (see Fig. 8a and d). In most semi-arid areas, where savanna grasslands dominate, resources are available to support forests which are suppressed by frequent fire (Bond and Keeley, 2005). Fire is thought to be the next most important driver of vegetation variation in savannas after precipitation (Sankaran et al., 2005).

Although northern and southern African semi-arid drylands experience similar increasing trends in precipitation (Fig. 9a), the changes in the vegetation indices are very different. In southern Africa (i.e., south of 5°S), NDVI trends are declining, while VOD trends are increasing; likely caused by an increase in woody component. Northern African savannas (in contrast with the grasslands in adjacent arid drylands), show increasing trends in NDVI, along with increasing trends (in most regions) for VOD; interpreted as an increase in the herbaceous component and/or increase in total AGB.

**BGD**

10, 8749–8797, 2013

## Global changes in dryland vegetation dynamics

N. Andela et al.

Title Page

Abstract

Introduction

Conclusions

References

Tables

Figures

◀

▶

◀

▶

Back

Close

Full Screen / Esc

Printer-friendly Version

Interactive Discussion



## Global changes in dryland vegetation dynamics

N. Andela et al.

Title Page

Abstract

Introduction

Conclusions

References

Tables

Figures



Back

Close

Full Screen / Esc

Printer-friendly Version

Interactive Discussion



The increasing trend in the north African grasslands and savannas is widely discussed in literature and has been explained as a result of recovery after drought (1983–1985 being the driest years; Anyamba and Tucker, 2005) and improved land management (e.g., irrigation, and soil and water conservation; Herrmann et al., 2005). Observed increases in wet season length in semi-arid parts of the region likely cause increasing trends, especially in NDVI (de Jong et al., 2011). Strong trends in NDVI occur in semi-arid areas with large annual burned area (compare Fig. 7e with Fig. 9d). Northern African savannas, with recent declines in annual burned area (Fig. 9b), showed increasing NDVI values (Fig. 7e). Widespread grazing (Fig. 9c) and associated fire suppression, may explain decreasing annual burned area in northern Africa between 2001 and 2011 (Fig. 9b; Archibald et al., 2010). Southern African regions, with recent increases in annual burned area, showed declining NDVI trends. We found that annual variation in burned area especially affects NDVI and VOD minimum values (Fig. 10). Human land use practice is also thought to be an important driver of annual burned area (Archibald et al., 2009). The effect of fire on vegetation indices is most profound in African and Australian savannas and woody savannas, where annual burned area typically ranges from 20 to 80% (Fig. 9d). In areas of high Net Primary Production (NPP), fire limits vegetation growth in the dry seasons, while in areas of low NPP fire is limited by NPP of the preceding season(s). Given the high percentage of area burnt each year in many African savannas and woody savannas (Fig. 10), it seems feasible that changing fire regimes, affecting annual minimum values of NDVI cause the observed trend in NDVI.

Outside the African savannas and woody savannas, the residual trends in NDVI are not easily attributed to changes in annual burned area, at least not using the data available to us. While even in the less fire prone regions, fire might play a crucial role in species competition, the direct effect of the smaller relative area of fire scars on the vegetation indices would be limited. Other drivers also affect vegetation dynamics, with the impact of fire on vegetation dynamics in other land cover types being less pronounced than in savannas (Fig. 10). NDVI can also be affected by grazing; while

any given area might support livestock during most times, the highest pressure on vegetation occurs during longer dry seasons. The negative trends in NDVI and VOD over the South American dry forests are likely caused by deforestation, that is reducing the woody vegetation component and therefore total AGB (Grau et al., 2005).

Trends in VOD occurred in areas of frequent fire, but no coherent spatial pattern was apparent (compare Fig. 7f with Fig. 9b and 9d). Although fire suppresses woody encroachment, dryland fires generally have a relatively low temperature and flame height and therefore do not necessarily affect established woody vegetation (Bond and Keeley, 2005). Woody vegetation increased in the southern African savannas despite increased burning (Figs. 9b and 11). This may be explained by increasing precipitation (Fig. 7; Sankaran et al., 2005), CO<sub>2</sub> fertilization (Buitenwerf et al., 2011; Higgins and Scheiter, 2012) and/or grazing by non domesticated herbivores. A clear increasing NDVI and VOD trend was found for croplands and adjacent grasslands in the USA. Woody encroachment in US grasslands has been widely reported (see Archer et al., 2001, and the references therein) and although there is no straightforward single driver, grazing is understood to play an important role (Van Auken, 2000; Briggs et al., 2005). Increasing agricultural activity could however also play a role in explaining those trends (Neigh et al., 2008).

The strongest positive median NDVI and VOD trends were found in agricultural areas (Fig. 8). Increases of both indices over the world's agricultural regions are explained by advances in agricultural practice including mechanization, irrigation and fertilization (Liu et al., 2013a). In India, Pakistan, Bangladesh, China, Ukraine, southwestern Russia, several European countries, the USA, and a number of other countries, substantial areas of agricultural land are irrigated (Wada et al., 2010). Evidence that increasing trends in NDVI are caused by irrigation and fertilization has been documented for India (Jeyaseelan et al., 2007) and the North China Plain (Piao et al., 2003), while Liu et al. (2013a) showed that positive VOD trends in southern Russia, China, India and the US are the result of increased agricultural production. In drylands at higher latitudes both water and temperature are factors limiting vegetation growth (Nemani et al., 2003), and

**BGD**

10, 8749–8797, 2013

## Global changes in dryland vegetation dynamics

N. Andela et al.

Title Page

Abstract

Introduction

Conclusions

References

Tables

Figures



Back

Close

Full Screen / Esc

Printer-friendly Version

Interactive Discussion





trends in these areas. Limited observations of monthly burned area suggests that after precipitation, changing fire regimes are an important driver of vegetation change in semi-arid drylands, especially in savannas.

6. Large changes in vegetation density were observed in agricultural dryland regions, where advances in agricultural practices caused increasing trends in both vegetation indices.

In summary, we demonstrated that using two complementary vegetation indices provide new insights into the dynamics of different vegetation components in global drylands. While it remains challenging to conclusively attribute dryland vegetation dynamics to any individual driver, a linear precipitation response model showed that change cannot be attributed to precipitation alone. Global data on fire regimes and grazing enabled a first assessment of the likely relative importance of these drivers on global vegetation change. Future improvements and extensions to time series of fire characteristics, grazing and land use change are likely to further improve understanding of global vegetation changes and its drivers.

*Acknowledgements.* The authors thank Jorge E. Pinzon and C. Jim Tucker (both with NASA, Biospheric Science Branch, Goddard Space Flight Center, Maryland, USA) for providing access to the NDVI GIMMS3g dataset (1981–2010).

## References

- Adamoli, J., Sennhauser, E., Acero, J. M., and Rescia, A.: Stress and disturbance: vegetation dynamics in the dry Chaco region of Argentina, *J. Biogeogr.*, 17, 491–500, 1990. 8767
- Allen, C. D., Macalady, A. K., Chenchouni, H., Bachelet, D., McDowell, N., Vennetier, M., Kitzberger, T., Rigling, A., Breshears, D. D., Hogg, E. H., Gonzalez, P., Fensham, R., Zhang, Z., Castro, J., Demidova, N., Lim, J. H., Allard, G., Running, S. W., Semerci, A., and Cobb, N.: A global overview of drought and heat-induced tree mortality reveals emerging climate change risks for forests, *Forest Ecol. Manage.*, 259, 660–684, 2010. 8770

BGD

10, 8749–8797, 2013

## Global changes in dryland vegetation dynamics

N. Andela et al.

Title Page

Abstract

Introduction

Conclusions

References

Tables

Figures

⏪

⏩

◀

▶

Back

Close

Full Screen / Esc

Printer-friendly Version

Interactive Discussion



## Global changes in dryland vegetation dynamics

N. Andela et al.

Title Page

Abstract

Introduction

Conclusions

References

Tables

Figures



Back

Close

Full Screen / Esc

Printer-friendly Version

Interactive Discussion



- Anyamba, A. and Tucker, C. J.: Analysis of Sahelian vegetation dynamics using NOAA-AVHRR NDVI data from 1981–2003, *J. Arid Environ.*, 63, 596–614, 2005. 8772
- Archer, S., Schimel, D. S., and Holland, E. A.: Mechanisms of shrubland expansion: land use, climate or CO<sub>2</sub>?, *Climatic Change*, 29, 91–99, 1995. 8751, 8752
- 5 Archer, S., Boutton, T. W., and Hibbard, K. A.: Trees in grasslands: biogeochemical consequences of woody plant expansion, In: *Global Biogeochemical Cycles in the Climate System*, 115–138, Academic Pres, San Diego, 2001. 8767, 8773
- Archibald, S. and Scholes, R. J.: Leaf green-up in a semi-arid African savanna-separating tree and grass responses to environmental cues, *J. Veg. Sci.*, 18, 583–594, 2007. 8753, 8768, 8770
- 10 Archibald, S., Roy, D. P., van Wilgen, B. W., and Scholes, R. J.: What limits fire? An examination of drivers of burnt area in Southern Africa, *Glob. Change Biol.*, 15, 613–630, 2009. 8769, 8772
- Archibald, S., Scholes, R. J., Roy, D. P., Roberts, G., and Boschetti, L.: Southern African fire regimes as revealed by remote sensing, *Int. J. Wildland Fire*, 19, 861–878, 2010. 8751, 8752, 8772
- 15 Asner, G. P.: Biophysical and biochemical sources of variability in canopy reflectance, *Remote Sens. Environ.*, 64, 234–253, 1998. 8755
- Asner, G. P., Borghi, C. E., and Ojeda, R. A.: Desertification in central Argentina: changes in ecosystem carbon and nitrogen from imaging spectroscopy, *Ecol. Appl.*, 13, 629–648, 2003. 8752
- 20 Asner, G. P., Elmore, A. J., Olander, L. P., Martin, R. E., and Harris, A. T.: Grazing systems, ecosystem responses, and global change, *Annu. Rev. Env. Resour.*, 29, 261–299, 2004. 8751, 8752, 8769, 8770
- 25 Asrar, G., Fuchs, M., Kanemasu, E. T., and Hatfield, J. L.: Estimating absorbed photosynthetic radiation and leaf area index from spectral reflectance in wheat, *Agron. J.*, 76, 300–306, 1984. 8752
- Bai, Z. G., Dent, D. L., Olsson, L., and Schaepman, M. E.: Proxy global assessment of land degradation, *Soil Use Manage.*, 24, 223–234, 2008. 8751, 8753, 8770
- 30 Beck, H. E., McVicar, T. R., van Dijk, A. I. J. M., Schellekens, J., de Jeu, R. A. M., and Bruijnzeel, L. A.: Global evaluation of four AVHRR-NDVI data sets: Intercomparison and assessment against Landsat imagery, *Remote Sens. Environ.*, 115, 2547–2563, 2011. 8752, 8757

## Global changes in dryland vegetation dynamics

N. Andela et al.

Title Page

Abstract

Introduction

Conclusions

References

Tables

Figures



Back

Close

Full Screen / Esc

Printer-friendly Version

Interactive Discussion



- Bond, W. J. and Keeley, J. E.: Fire as a global 'herbivore': the ecology and evolution of flammable ecosystems, *Trends Ecol. Evol.*, 20, 387–394, 2005. 8751, 8752, 8771, 8773
- Bond, W. J. and Midgley, G. F.: Carbon dioxide and the uneasy interactions of trees and savannah grasses, *Philos. T. R. Soc. B*, 367, 601–612, 2012. 8751, 8752, 8770
- 5 Bond, W. J., Midgley, G. F., and Woodward, F. I.: The importance of low atmospheric CO<sub>2</sub> and fire in promoting the spread of grasslands and savannas, *Glob. Change Biol.*, 9, 973–982, 2003. 8751, 8761
- Bond, W. J., Woodward, F. I., and Midgley, G. F.: The global distribution of ecosystems in a world without fire, *New Phytol.*, 165, 525–538, 2005. 8752
- 10 Bowman, D. M. J. S., Balch, J. K., Artaxo, P., Bond, W. J., Carlson, J. M., Cochrane, M. A., D'Antonio, C. M., DeFries, R. S., Doyle, J. C., Harrison, S. P., Johnston, F. H., Keeley, J. E., Krawchuk, M. A., Kull, C. A., Marston, J. B., Moritz, M. A., Prentice, I. C., Roos, C. I., Scott, A. C., Swetnam, T. W., Werf, v. d. G. R., and Pyne, S. J.: Fire in the Earth system, *Science*, 324, 481–484, 2009. 8752, 8769
- 15 Breshears, D. D.: The grassland-forest continuum: trends in ecosystem properties for woody plant mosaics?, *Front. Ecol. Environ.*, 4, 96–104, 2006. 8770
- Briggs, J. M., Knapp, A. K., Blair, J. M., Heisler, J. L., Hoch, G. A., Lett, M. S., and McCarron, J. K.: An ecosystem in transition: causes and consequences of the conversion of mesic grassland to shrubland, *BioScience*, 55, 243–254, 2005. 8773
- 20 Brooks, M. L., D'Antonio, C. M., Richardson, D. M., Grace, J. B., Keeley, J. E., DiTomaso, J. M., Hobbs, R. J., Pellant, M., and Pyke, D.: Effects of invasive alien plants on fire regimes, *BioScience*, 54, 677–688, 2004. 8770
- Brown, M. E., Pinzón, J. E., Didan, K., Morisette, J. T., and Tucker, C. J.: Evaluation of the consistency of long-term NDVI time series derived from AVHRR, SPOT-Vegetation, SeaWiFS, MODIS, and Landsat ETM+ sensors, *IEEE T. Geosci. Remote*, 44, 1787–1793, 2006. 8757, 8762
- 25 Buitenwerf, R., Bond, W. J., Stevens, N., and Trollope, W. S. W.: Increased tree densities in South African savannas: > 50 years of data suggests CO<sub>2</sub> as a driver, *Glob. Change Biol.*, 18, 675–684, 2011. 8752, 8769, 8773
- 30 Carlson, T. N. and Ripley, D. A.: On the relation between NDVI, fractional vegetation cover, and leaf area index, *Remote Sens. Environ.*, 62, 241–252, 1997. 8752
- de Jeu, R. A. M.: Retrieval of Land Surface Parameters using Passive Microwave Remote Sensing, Ph.D. thesis, VU University, Amsterdam, 2003. 8758

## Global changes in dryland vegetation dynamics

N. Andela et al.

[Title Page](#)

[Abstract](#)

[Introduction](#)

[Conclusions](#)

[References](#)

[Tables](#)

[Figures](#)

[◀](#)

[▶](#)

[◀](#)

[▶](#)

[Back](#)

[Close](#)

[Full Screen / Esc](#)

[Printer-friendly Version](#)

[Interactive Discussion](#)



- de Jong, R., de Bruin, S., de Wit, A., Schaepman, M. E., and Dent, D. L.: Analysis of monotonic greening and browning trends from global NDVI time-series, *Remote Sens. Environ.*, 115, 692–702, 2011. 8751, 8753, 8761, 8770, 8772
- Díaz-Delgado, R., Lloret, F., and Pons, X.: Influence of fire severity on plant regeneration by means of remote sensing imagery, *Int. J. Remote Sens.*, 24, 1751–1763, 2003. 8769
- Donohue, R. J., McVicar, T. R., and Roderick, M. L.: Climate-related trends in Australian vegetation cover as inferred from satellite observations, 1981–2006, *Glob. Change Biol.*, 15, 1025–1039, 2009. 8751, 8753, 8755, 8768
- Donohue, R. J., Roderick, M. L., McVicar, T. R., and Farquhar, G. D.: CO<sub>2</sub> fertilisation has increased maximum foliage cover across the globe's warm, arid environments, *Geophys. Res. Lett.*, accepted, doi:10.1002/grl.50563, 2013. 8751, 8761, 8770
- Dore, M. H. I.: Climate change and changes in global precipitation patterns: What do we know?, *Environ. Int.*, 31, 1167–1181, 2005. 8751
- Drake, B. G., González-Meler, M. A., and Long, S. P.: More efficient plants: a consequence of rising atmospheric CO<sub>2</sub>?, *Ann. Rev. Plant Biol.*, 48, 609–639, 1997. 8770
- Evans, J. and Geerken, R.: Discrimination between climate and human-induced dryland degradation, *J. Arid Environ.*, 57, 535–554, 2004. 8751, 8753, 8760, 8768
- Farquhar, G. D.: Carbon dioxide and vegetation, *Science*, 278, 1411–1411, 1997. 8770
- Fensham, R. J., Fairfax, R. J., and Archer, S. R.: Rainfall, land use and woody vegetation cover change in semi-arid Australian savanna, *J. Ecol.*, 93, 596–606, 2005. 8752, 8767, 8769
- Fensholt, R., Langanke, T., Rasmussen, K., Reenberg, A., Prince, S. D., Tucker, C. J., Scholes, R. J., Bao Le, Q., Bondeau, A., Eastman, R., Epstein, H., Gaughan, A. E., Hellden, U., Mbow, C., Olsson, L., Paruelo, J., Schweitzer, C., Seaquist, J., and Wessels, K.: Greenness in semi-arid areas across the globe 1981–2007 – an Earth Observing Satellite based analysis of trends and drivers, *Remote Sens. Environ.*, 121, 144–158, 2012. 8751, 8753, 8761
- Flannigan, M. D., Krawchuk, M. A., De Groot, W. J., Wotton, B. M., and Gowman, L. M.: Implications of changing climate for global wildland fire, *Int. J. Wildland Fire*, 18, 483–507, 2009. 8752
- Giglio, L., Loboda, T., Roy, D. P., Quayle, B., and Justice, C. O.: An active-fire based burned area mapping algorithm for the MODIS sensor, *Remote Sens. Environ.*, 113, 408–420, 2009. 8758
- Gouweleeuw, B. T., van Dijk, A. I. J. M., Guerschman, J. P., Dyce, P., and Owe, M.: Space-based passive microwave soil moisture retrievals and the correction for a dynamic open water

fraction, *Hydrol. Earth Syst. Sci.*, 16, 1635–1645, doi:10.5194/hess-16-1635-2012, 2012. 8758

Grau, H. R., Gasparri, N. I., and Aide, T. M.: Agriculture expansion and deforestation in seasonally dry forests of north-west Argentina, *Environ. Conserv.*, 32, 140–148, 2005. 8773

Hansen, M. C., DeFries, R. S., Townshend, J. R. G., and Sohlberg, R.: Global land cover classification at 1 km spatial resolution using a classification tree approach, *Int. J. Remote Sens.*, 21, 1331–1364, 2000. 8758

Heisler, J. L., Briggs, J. M., and Knapp, A. K.: Long-term patterns of shrub expansion in a C4-dominated grassland: fire frequency and the dynamics of shrub cover and abundance, *Am. J. Bot.*, 90, 423–428, 2003. 8752

Herrmann, S. M., Anyamba, A., and Tucker, C. J.: Recent trends in vegetation dynamics in the African Sahel and their relationship to climate, *Global Environmental Change Part A*, 15, 394–404, 2005. 8751, 8753, 8760, 8761, 8768, 8772

Higgins, S. I. and Scheiter, S.: Atmospheric CO<sub>2</sub> forces abrupt vegetation shifts locally, but not globally, *Nature*, 488, 209–212, 2012. 8770, 8771, 8773

Hijmans, R. J., Cameron, S. E., Parra, J. L., Jones, P. G., and Jarvis, A.: Very high resolution interpolated climate surfaces for global land areas, *Int. J. Climatol.*, 25, 1965–1978, 2005.

House, J. I., Archer, S., Breshears, D. D., and Scholes, R. J.: Conundrums in mixed woody-herbaceous plant systems, *J. Biogeogr.*, 30, 1763–1777, 2003. 8768

Jackson, T. J., Schmugge, T. J., and Wang, J. R.: Passive microwave sensing of soil moisture under vegetation canopies, *Water Resour. Res.*, 18, 1137–1142, 1982. 8755

Jahnke, H. E.: Livestock production systems and livestock development in tropical Africa, Kieler Wissenschaftsverlag Vauk: Kiel, available from: [http://pdf.usaid.gov/pdf\\_docs/pnaan484.pdf](http://pdf.usaid.gov/pdf_docs/pnaan484.pdf), 1982. 8759

Jeyaseelan, A. T., Roy, P. S., and Young, S. S.: Persistent changes in NDVI between 1982 and 2003 over India using AVHRR GIMMS (Global Inventory Modeling and Mapping Studies) data, *Int. J. Remote Sens.*, 28, 4927–4946, 2007. 8751, 8773

Jones, M. O., Jones, L. A., Kimball, J. S., and McDonald, K. C.: Satellite passive microwave remote sensing for monitoring global land surface phenology, *Remote Sens. Environ.*, 115, 1102–1114, 2011. 8753, 8758, 8766

Jones, M. O., Kimball, J. S., Jones, L. A., and McDonald, K. C.: Satellite passive microwave detection of North America start of season, *Remote Sens. Environ.*, 123, 324–333, 2012. 8753

**BGD**

10, 8749–8797, 2013

## Global changes in dryland vegetation dynamics

N. Andela et al.

Title Page

Abstract

Introduction

Conclusions

References

Tables

Figures

◀

▶

◀

▶

Back

Close

Full Screen / Esc

Printer-friendly Version

Interactive Discussion



## Global changes in dryland vegetation dynamics

N. Andela et al.

Title Page

Abstract

Introduction

Conclusions

References

Tables

Figures

◀

▶

◀

▶

Back

Close

Full Screen / Esc

Printer-friendly Version

Interactive Discussion



Jones, P. and Harris, I.: CRU Time Series (TS) high resolution gridded datasets, university of East Anglia Research Unit (CRU) NCAS British Atmospheric Data Centre, available from [http://badc.nerc.ac.uk/view/badc.nerc.ac.uk\\_\\_ATOM\\_\\_dataent\\_1256223773328276](http://badc.nerc.ac.uk/view/badc.nerc.ac.uk__ATOM__dataent_1256223773328276), 2008. 8758

5 Kaufman, Y. J., Justice, C. O., Flynn, L. P., Kendall, J. D., Prins, E. M., Giglio, L., Ward, D. E., Menzel, W. P., and Setzer, A. W.: Potential global fire monitoring from EOS-MODIS, *J. Geophys. Res.*, 103, 32 215–32, 1998. 8752

Kirdiashev, K. P., Chukhlantsev, A. A., and Shutko, A. M.: Microwave radiation of the Earth's surface in the presence of vegetation cover, *Radio Eng. Electron. P.*, 24, 37–44, 1979. 8752

10 Lehmann, C. E. R., Archibald, S. A., Hoffmann, W. A., and Bond, W. J.: Deciphering the distribution of the savanna biome, *New Phytol.*, 191, 197–209, 2011. 8752, 8769

Liu, Y. Y., de Jeu, R. A. M., van Dijk, A. I. J. M., and Owe, M.: TRMM-TMI satellite observed soil moisture and vegetation density (1998–2005) show strong connection with El Niño in eastern Australia, *Geophys. Res. Lett.*, 34, L15401, doi:10.1029/2007GL030311, 2007. 8753

15 Liu, Y. Y., de Jeu, R. A. M., McCabe, M. F., Evans, J. P., and van Dijk, A. I. J. M.: Global long-term passive microwave satellite-based retrievals of vegetation optical depth, *Geophys. Res. Lett.*, 38, L18402, doi:10.1029/2011GL048684, 2011a. 8753, 8757, 8759, 8762, 8766

Liu, Y. Y., Parinussa, R. M., Dorigo, W. A., De Jeu, R. A. M., Wagner, W., van Dijk, A. I. J. M., McCabe, M. F., and Evans, J. P.: Developing an improved soil moisture dataset by blending passive and active microwave satellite-based retrievals, *Hydrol. Earth Syst. Sci.*, 15, 425–436, doi:10.5194/hess-15-425-2011, 2011b. 8757

Liu, Y. Y., Dijk, A. I. J. M., McCabe, M. F., Evans, J. P., and de Jeu, R. A. M.: Global vegetation biomass change (1988–2008) and attribution to environmental and human drivers, *Global Ecol. Biogeogr.*, 22, 692–705, doi:10.1111/geb.12024, 2013a. 8751, 8753, 8757, 8761, 8773

25 Liu, Y. Y., Evans, J. P., McCabe, M. F., de Jeu, R. A. M., van Dijk, A. I. J. M., Dolman, A. J., and Saizen, I.: Changing Climate and Overgrazing Are Decimating Mongolian Steppes, *PLoS one*, 8, e57599, doi:10.1371/journal.pone.0057599, 2013b. 8751, 8753

Lu, H., Raupach, M. R., McVicar, T. R., and Barrett, D. J.: Decomposition of vegetation cover into woody and herbaceous components using AVHRR NDVI time series, *Remote Sens. Environ.*, 86, 1–18, 2003. 8752, 8753, 8755

30 McMahan, S. M., Parker, G. G., and Miller, D. R.: Evidence for a recent increase in forest growth, *P. Natl. Acad. Sci. USA*, 107, 3611–3615, 2010. 8752



## Global changes in dryland vegetation dynamics

N. Andela et al.

Title Page

Abstract

Introduction

Conclusions

References

Tables

Figures

◀

▶

◀

▶

Back

Close

Full Screen / Esc

Printer-friendly Version

Interactive Discussion



- Owe, M., de Jeu, R. A. M., and Holmes, T. R. H.: Multi-Sensor Historical Climatology of Satellite-Derived Global Land Surface Moisture, *J. Geophys. Res.*, 113, F01002, doi:10.1029/2007JF000769, 2008. 8753
- Pettorelli, N., Vik, J. O., Mysterud, A., Gaillard, J. M., Tucker, C. J., and Stenseth, N. C.: Using the satellite-derived NDVI to assess ecological responses to environmental change, *Trends Ecol. Evol.*, 20, 503–510, 2005. 8753
- Piao, S. L., Fang, J. Y., Zhou, L. M., Guo, Q. H., Henderson, M., Ji, W., Li, Y., and Tao, S.: Inter-annual variations of monthly and seasonal normalized difference vegetation index (NDVI) in China from 1982 to 1999, *J. Geophys. Res.*, 108, 4401, doi:10.1029/2002JD002848, 2003. 8751, 8773
- Reich, P. B., Walters, M. B., and Ellsworth, D. S.: From tropics to tundra: global convergence in plant functioning, *P. Natl. Acad. Sci. USA*, 94, 13730–13734, 1997. 8755
- Reich, P. B., Wright, I. J., Cavender-Bares, J., Craine, J. M., Oleksyn, J., Westoby, M., and Walters, M. B.: The evolution of plant functional variation: traits, spectra, and strategies, *Int. J. Plant Sci.*, 164, S143–S164, 2003. 8755
- Robinson, T. P., Franceschini, G., and Wint, W.: The Food and Agriculture Organization's gridded livestock of the world, *Veterinaria Italiana*, 43, 745–751, 2007. 8759
- Roderick, M. L., Berry, S. L., Saunders, A. R., and Noble, I. R.: On the relationship between the composition, morphology and function of leaves, *Funct. Ecol.*, 13, 696–710, 1999a. 8755
- Roderick, M. L., Noble, I. R., and Cridland, S. W.: Estimating woody and herbaceous vegetation cover from time series satellite observations, *Global Ecol. Biogeogr.*, 8, 501–508, 1999b. 8753, 8755
- Roderick, M. L., Berry, S. L., and Noble, I. R.: A framework for understanding the relationship between environment and vegetation based on the surface area to volume ratio of leaves, *Funct. Ecol.*, 14, 423–437, 2000. 8755
- Rossatto, D. R., da Silveira Lobo Sternberg, L., and Franco, A. C.: The partitioning of water uptake between growth forms in a Neotropical savanna: do herbs exploit a third water source niche?, *Plant Biol.*, 15, 84–92, doi:10.1111/j.1438-8677.2012.00618.x, 2013. 8768
- Rouse, J. W., Haas, R. H., Schell, J. A., Deering, D. W., and Harlan, J. C.: Monitoring the vernal advancement of retrogradation of natural vegetation, NASA/GSFC, Tech. rep., Greenbelt, MD, 1974. 8752
- Sankaran, M., Hanan, N. P., Scholes, R. J., Ratnam, J., Augustine, D. J., Cade, B. S., Gignoux, J., Higgins, S. I., Le Roux, X., Ludwig, F., Ardo, J., Banyikwa, F., Bronn, A., Bucini, G., Caylor,



## Global changes in dryland vegetation dynamics

N. Andela et al.

[Title Page](#)

[Abstract](#)

[Introduction](#)

[Conclusions](#)

[References](#)

[Tables](#)

[Figures](#)



[Back](#)

[Close](#)

[Full Screen / Esc](#)

[Printer-friendly Version](#)

[Interactive Discussion](#)



- Tucker, C. J., Pinzon, J. E., Brown, M. E., Slayback, D. A., Pak, E. W., Mahoney, R., Vermote, E. F., and El Saleous, N.: An extended AVHRR 8-km NDVI dataset compatible with MODIS and SPOT vegetation NDVI data, *Int. J. Remote Sens.*, 26, 4485–4498, 2005. 8757
- 5 Van Auken, O. W.: Shrub invasions of North American semiarid grasslands, *Annu. Rev. Ecol. Syst.*, 31, 197–215, 2000. 8751, 8752, 8773
- Vegten, J. A.: Thornbush invasion in a savanna ecosystem in eastern Botswana, *Plant Ecol.*, 56, 3–7, 1984. 8767
- Wada, Y., van Beek, L. P. H., van Kempen, C. M., Reckman, J. W. T. M., Vasak, S., and Bierkens, M. F. P.: Global depletion of groundwater resources, *Geophys. Res. Lett.*, 37, L20402, doi:10.1029/2010GL044571, 2010. 8773
- 10 Wang, Q., Adiku, S., Tenhunen, J., and Granier, A.: On the relationship of NDVI with leaf area index in a deciduous forest site, *Remote Sens. Environ.*, 94, 244–255, 2005. 8752
- Wessels, K. J., Prince, S. D., Malherbe, J., Small, J., Frost, P. E., and VanZyl, D.: Can human-induced land degradation be distinguished from the effects of rainfall variability? A case study in South Africa, *J. Arid Environ.*, 68, 271–297, 2007. 8751, 8753, 8760, 8768, 8770
- 15 Wigneron, J. P., Kerr, Y., Chanzy, A., and Jin, Y. Q.: Inversion of surface parameters from passive microwave measurements over a soybean field, *Remote Sens. Environ.*, 46, 61–72, 1993. 8755
- Zomer, R. J., Trabucco, A., Bossio, D. A., and Verchot, L. V.: Climate change mitigation: A spatial analysis of global land suitability for clean development mechanism afforestation' and reforestation, *Agr. Ecosys. Environ.*, 126, 67–80, 2008.
- 20

## Global changes in dryland vegetation dynamics

N. Andela et al.

**Table 1.** Percentage of global drylands with significant ( $p < 0.05$ ) correlation between API and the two vegetation indices for land cover and humidity classes. The average humidity ( $P/ET_p$ ) for each land cover class is shown in brackets with the land cover classes ordered in increasing humidity. 1 % represents  $\approx 750$  grid cells ( $0.25^\circ$  resolution), abbreviations of land cover classes are explained in the legend of Fig. 1a.

Land cover				Humidity			
Class	Total [%]	NDVI [%]	VOD [%]	Class [%]	Total [%]	NDVI [%]	VOD [%]
B/SV (0.08)	12.7	7.1	8.4	0–0.1	12.2	6.7	8.2
Sh (0.31)	12.0	10.4	10.5	0.1–0.3	17.2	15.8	16.2
Gr (0.42)	14.1	11.6	11.8	0.3–0.5	13.4	11.9	11.8
Sa (0.60)	7.6	5.9	6.4	0.5–0.7	14.4	8.8	8.4
Cr (0.70)	15.7	10.3	9.1	0.7–0.9	14.5	6.6	6.1
WSa (0.81)	9.5	5.4	5.5	0.9–1.1	11.9	4.5	3.9
M/DF (0.93)	12.4	3.8	3.3	1.1–1.3	7.2	2.1	2.0
ENF (1.09)	5.9	1.1	1.3	> 1.3	9.1	3.2	2.8
EBF (1.39)	10.0	4.0	3.1				
Total	100.0	59.7	59.4	Total	100.0	59.7	59.4

[Title Page](#)
[Abstract](#)
[Introduction](#)
[Conclusions](#)
[References](#)
[Tables](#)
[Figures](#)
[Back](#)
[Close](#)
[Full Screen / Esc](#)
[Printer-friendly Version](#)
[Interactive Discussion](#)


## Global changes in dryland vegetation dynamics

N. Andela et al.

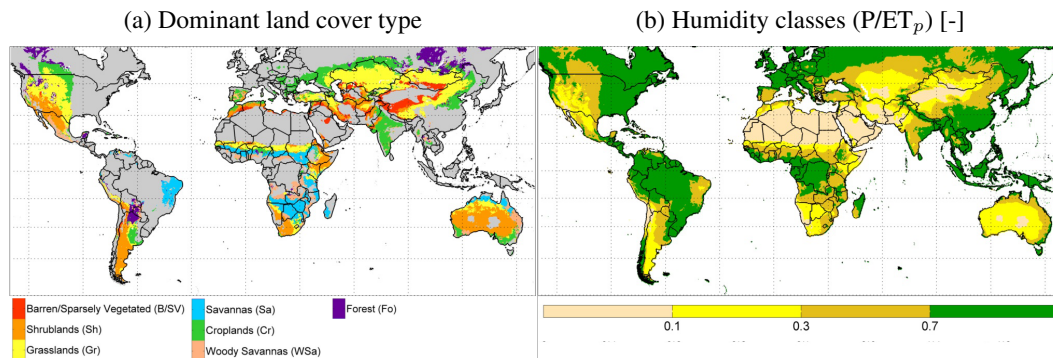


**Fig. 1.** Characterization of ecosystem in terms of land cover and humidity. **(a)** MODIS dominant land cover type, herein referred to as land cover; and **(b)** humidity classes, based on 50 yr average (1950–2000) precipitation ( $P$ ) data (Hijmans et al., 2005) and potential evaporation ( $ET_p$ ) data (Zomer et al., 2008). All maps in this paper (except for Fig. 3d) are projected in the Miller Cylindrical projection ( $60^\circ$  N– $60^\circ$  S,  $130^\circ$  W– $160^\circ$  E). Terrestrial areas that are not drylands ( $0.1 < \text{humidity} \leq 0.7$ ) are from now on masked grey in all figures and are excluded from analysis, and oceans are masked (white) in all figures.

Title Page

Abstract

Introduction

Conclusions

References

Tables

Figures

◀

▶

◀

▶

Back

Close

Full Screen / Esc

Printer-friendly Version

Interactive Discussion



Global changes in  
dryland vegetation  
dynamics

N. Andela et al.

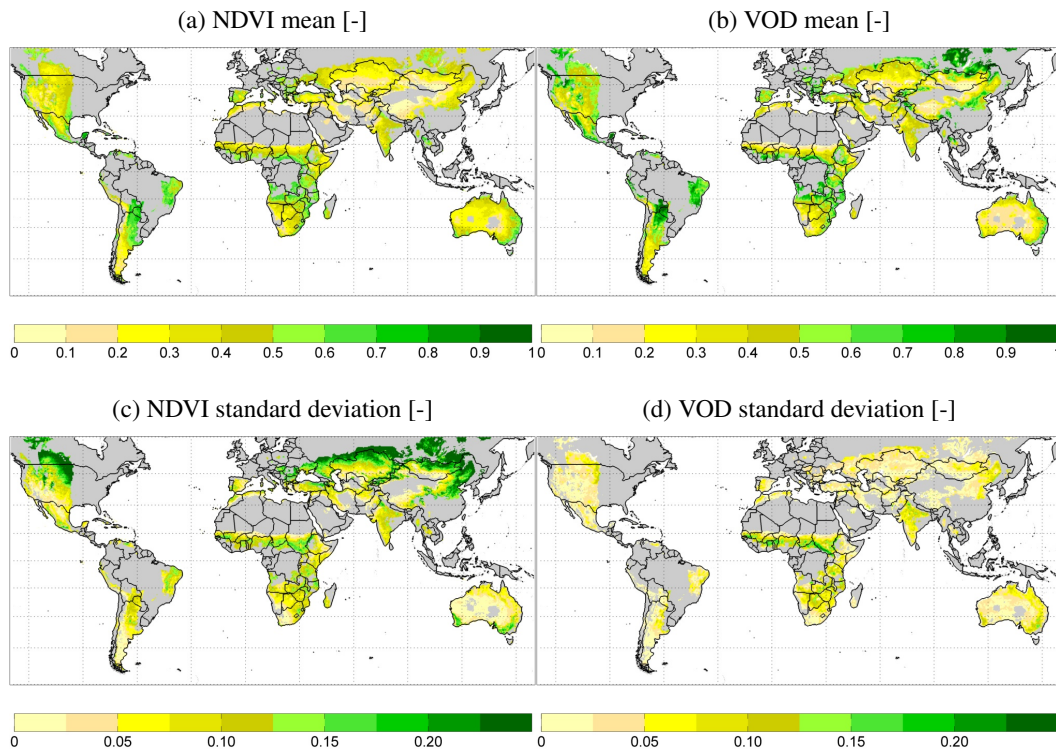


**Fig. 2.** Mean values and standard deviation of vegetation indices (1988–2008). **(a)** Mean NDVI; **(b)** mean VOD; **(c)** standard deviation of NDVI; and **(d)** standard deviation of VOD.

[Title Page](#)
[Abstract](#)
[Introduction](#)
[Conclusions](#)
[References](#)
[Tables](#)
[Figures](#)
[◀](#)
[▶](#)
[◀](#)
[▶](#)
[Back](#)
[Close](#)
[Full Screen / Esc](#)
[Printer-friendly Version](#)
[Interactive Discussion](#)


Global changes in  
dryland vegetation  
dynamics

N. Andela et al.

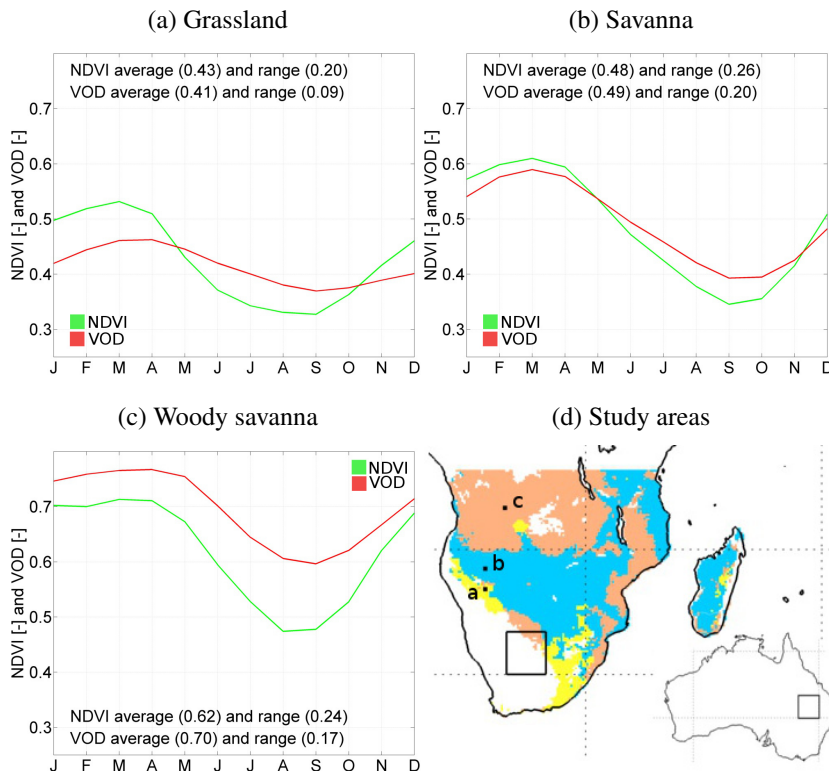


**Fig. 3.** Long-term (1988–2008) average monthly NDVI and VOD signals for three common land cover classes of southern Africa (5–35° S, 10–50° E): **(a)** grassland (733 0.25° resolution grid cells), **(b)** savanna (4041 0.25° resolution grid cells), and **(c)** woody savanna (3826 0.25° resolution grid cells). The annual average and range of both vegetation indices are reported on each sub-plot. **(d)** Shows an overview of the study areas used in Figs. 3, 6 and 10. Australia is shown at half the scale of southern Africa. The three regions, based on land cover, used in **(a–c)** are shown in yellow (grassland), blue (savanna) and pink (woody savanna).

Title Page

Abstract

Introduction

Conclusions

References

Tables

Figures

◀

▶

◀

▶

Back

Close

Full Screen / Esc

Printer-friendly Version

Interactive Discussion

## Global changes in dryland vegetation dynamics

N. Andela et al.

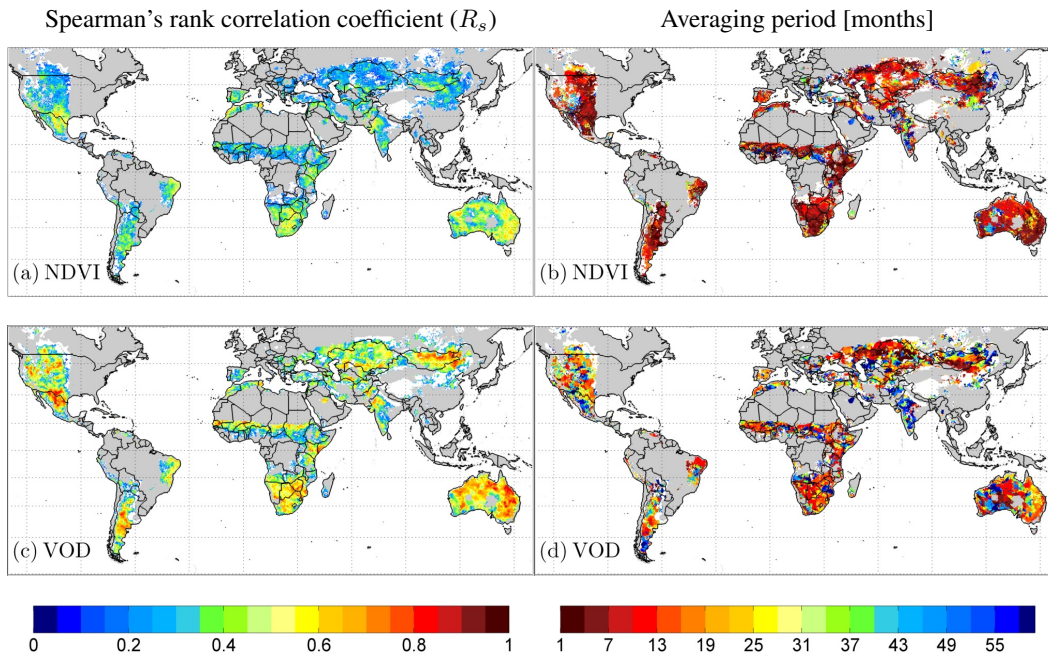


**Fig. 4.** Spearman's rank correlation coefficient ( $R_s$ ) and averaging periods for the two vegetation indices. For the NDVI **(a)** is the  $R_s$  between API and the NDVI anomaly and **(b)** is the averaging period for antecedent precipitation that leads to the highest  $R_s$  between PRM and the vegetation anomalies (denoted as  $T$  in the methods), **(c)** and **(d)** are as **(a)** and **(b)** except for the VOD. Grid cells without significant correlation ( $p < 0.05$ ), with over 60 % missing values, or with a negative correlation coefficients are masked (white).

Title Page

Abstract

Introduction

Conclusions

References

Tables

Figures

◀

▶

◀

▶

Back

Close

Full Screen / Esc

Printer-friendly Version

Interactive Discussion

## Global changes in dryland vegetation dynamics

N. Andela et al.

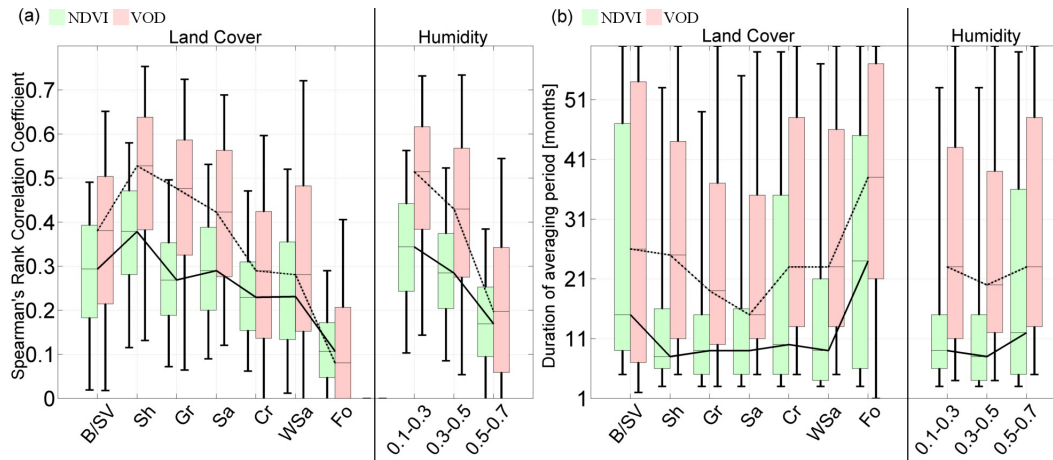


**Fig. 5.** Box plots showing the distribution of  $R_s$  and averaging periods for the two vegetation indices. **(a)** Distribution of  $R_s$  between observed vegetation anomalies and API for NDVI and VOD, stratified by: (left) land cover classes and (right) humidity classes; and **(b)** the distribution of the duration of averaging period for antecedent precipitation that leads to strongest correlation between the PRM and observed vegetation anomalies, stratified by: (left) land cover classes and (right) humidity classes. Solid lines indicate the NDVI medians and dash-dot lines the VOD medians. The maximum and minimum extents of the colored boxes indicate 25th and 75th percentiles and whiskers represent the 5th and 95th percentiles. Grid cells with over 60% missing values are not included in this figure, and grid cells without significant correlation ( $p > 0.05$ ) in Fig. 4 are not included in Fig. 5b. Abbreviations of land cover classes are explained in the legend of Fig. 1a.

Title Page

Abstract

Introduction

Conclusions

References

Tables

Figures

◀

▶

◀

▶

Back

Close

Full Screen / Esc

Printer-friendly Version

Interactive Discussion



## Global changes in dryland vegetation dynamics

N. Andela et al.

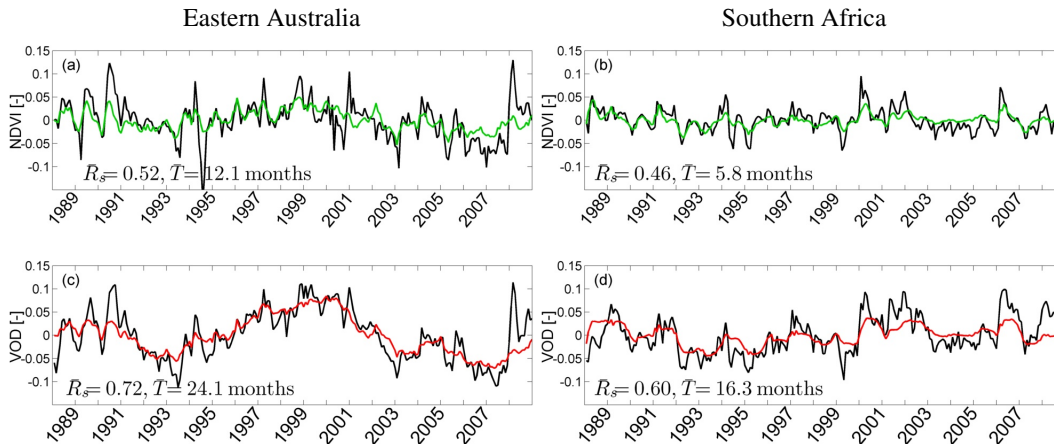


**Fig. 6.** Time series of expected and observed vegetation anomalies. Expected NDVI (green) and observed NDVI (black) vegetation anomalies are shown for regions in **(a)** eastern Australia (25–30° S, 145–150° E) and **(b)** southern Africa (25–30° S, 20–25° E), **(c)** and **(d)** are as **(a)** and **(b)** except for the expected VOD (red) and observed VOD (black) vegetation anomalies. The average Spearman's ranked correlation coefficient ( $R_s$ ) and averaging period ( $T$ ) of all 0.25° resolution grid cells in each 5° region are listed in each sub-plot. Locations of both 5° regions are shown in Fig. 3d.

Title Page

Abstract

Introduction

Conclusions

References

Tables

Figures

◀

▶

◀

▶

Back

Close

Full Screen / Esc

Printer-friendly Version

Interactive Discussion



## Global changes in dryland vegetation dynamics

N. Andela et al.

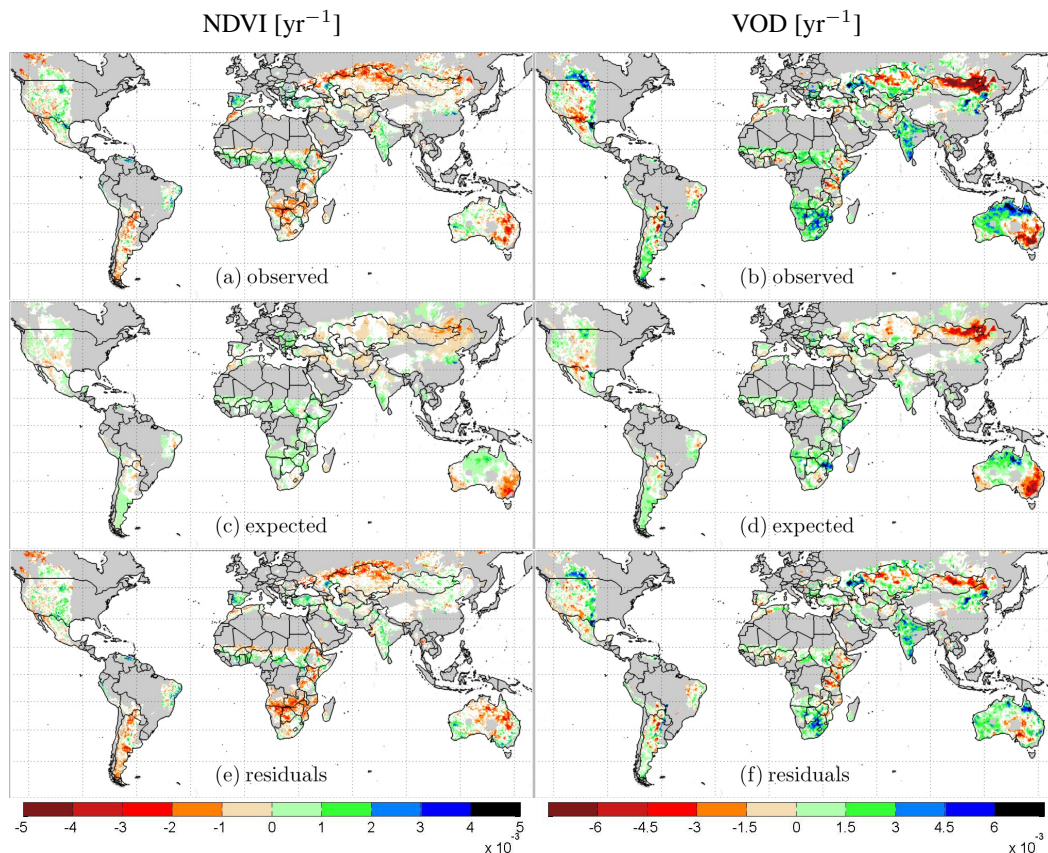


**Fig. 7.** Linear trends (1988–2008) of the observed, expected and residual for both vegetation indices: **(a)** and **(b)** are the NDVI and VOD observed trends, **(c)** and **(d)** are the NDVI and VOD expected trends, and **(e)** and **(f)** are the NDVI and VOD residual trends. Grid cells with over 60% missing values or without significant trends ( $p > 0.05$ ) are masked (white).

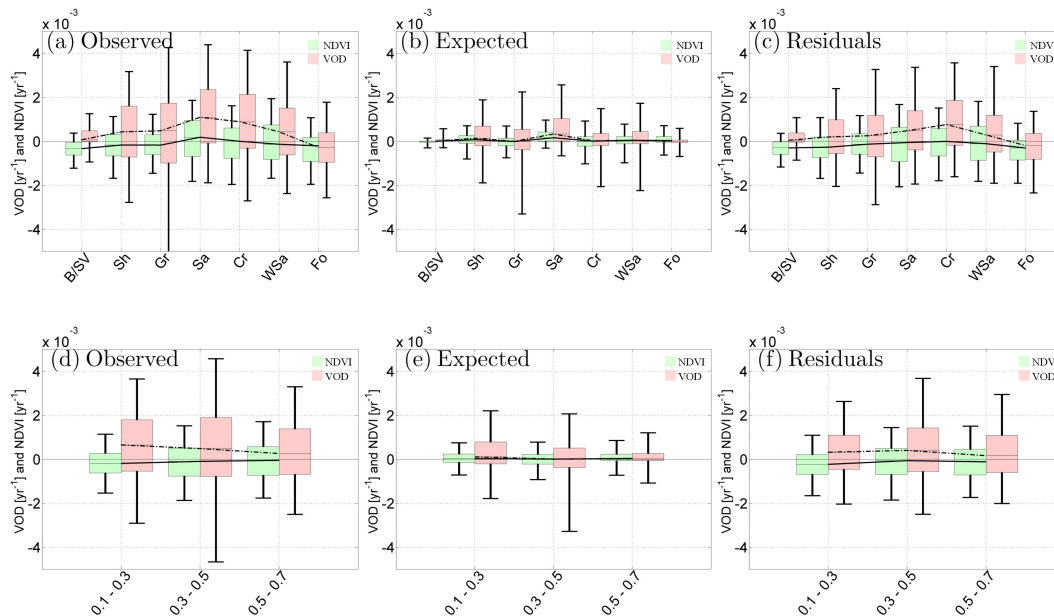


**Fig. 8.** Box plots of the distribution of observed, expected and residual linear trends for both vegetation indices. Observed trends stratified by the (a) land cover and (d) humidity classes, expected trends stratified by the (b) land cover and (e) humidity classes, and the residual trends stratified by the (c) land cover and (f) humidity classes. Solid lines indicate the NDVI medians and dash-dot lines the VOD medians. The maximum and minimum extents of the colored boxes indicate 25th and 75th percentiles and whiskers represent the 5th and 95th percentiles. Grid cells with over 60% missing values are not included in this figure. Abbreviations of land cover classes are explained in the legend of Fig. 1a.

[Title Page](#)
[Abstract](#)
[Introduction](#)
[Conclusions](#)
[References](#)
[Tables](#)
[Figures](#)
[Back](#)
[Close](#)
[Full Screen / Esc](#)
[Printer-friendly Version](#)
[Interactive Discussion](#)


## Global changes in dryland vegetation dynamics

N. Andela et al.

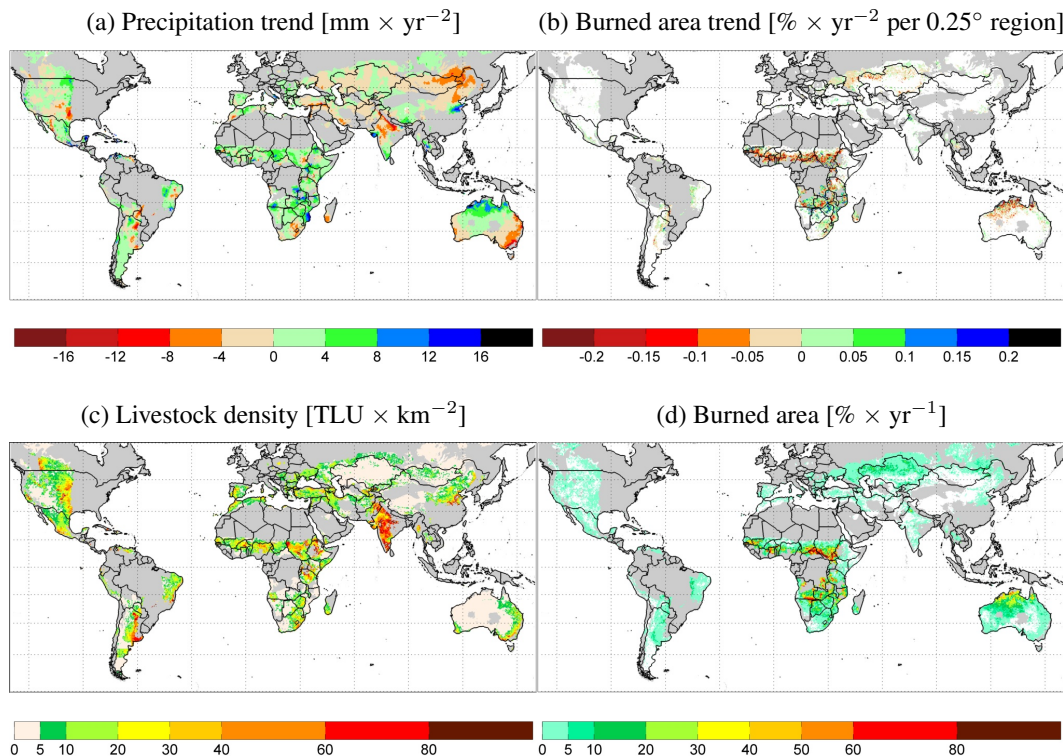


**Fig. 9.** Datasets used for interpretation of vegetation dynamics: **(a)** linear trend in annual mean precipitation (1988–2008), **(b)** linear trend in annual mean burned area (2001–2011), **(c)** livestock density, and **(d)** mean annual burned area (2001–2011). Due to MODIS data limitations the burned area trends are calculated from 2001–2011. Trends in burned area were only calculated for grid cells with burned area in at least 6 out of 11 yr, remaining grid cells are shown in white. For mean burned area **(d)**, grid cells with no fire occurrence (mean is zero) are shown in white. Trends are shown for all significance levels.

Title Page

Abstract

Introduction

Conclusions

References

Tables

Figures

◀

▶

◀

▶

Back

Close

Full Screen / Esc

Printer-friendly Version

Interactive Discussion



## Global changes in dryland vegetation dynamics

N. Andela et al.

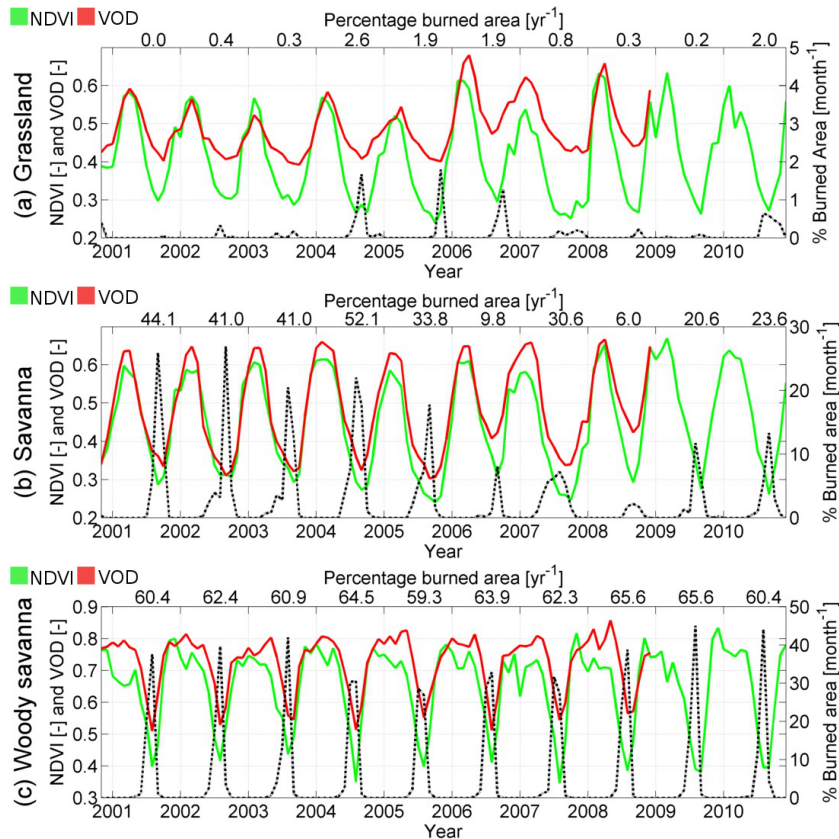


**Fig. 10.** Time series of NDVI, VOD and burned area (black, dashed) for three selected  $0.5^\circ$  regions with different land cover in southern Africa: **(a)** grassland ( $19.5\text{--}20.0^\circ\text{S}$ ,  $17.0\text{--}17.5^\circ\text{E}$ ), **(b)** savanna ( $17.0\text{--}17.5^\circ\text{S}$ ,  $17.0\text{--}17.5^\circ\text{E}$ ), and **(c)** woody savanna ( $9.5\text{--}10.0^\circ\text{S}$ ,  $19.5\text{--}20.0^\circ\text{E}$ ). Numbers above the sub-parts are the percentage burned area [ $\text{yr}^{-1}$ ], and locations of study areas are shown as black dots (marked a, b and c) within Fig. 3d.

Title Page

Abstract

Introduction

Conclusions

References

Tables

Figures

◀

▶

◀

▶

Back

Close

Full Screen / Esc

Printer-friendly Version

Interactive Discussion

## Global changes in dryland vegetation dynamics

N. Andela et al.

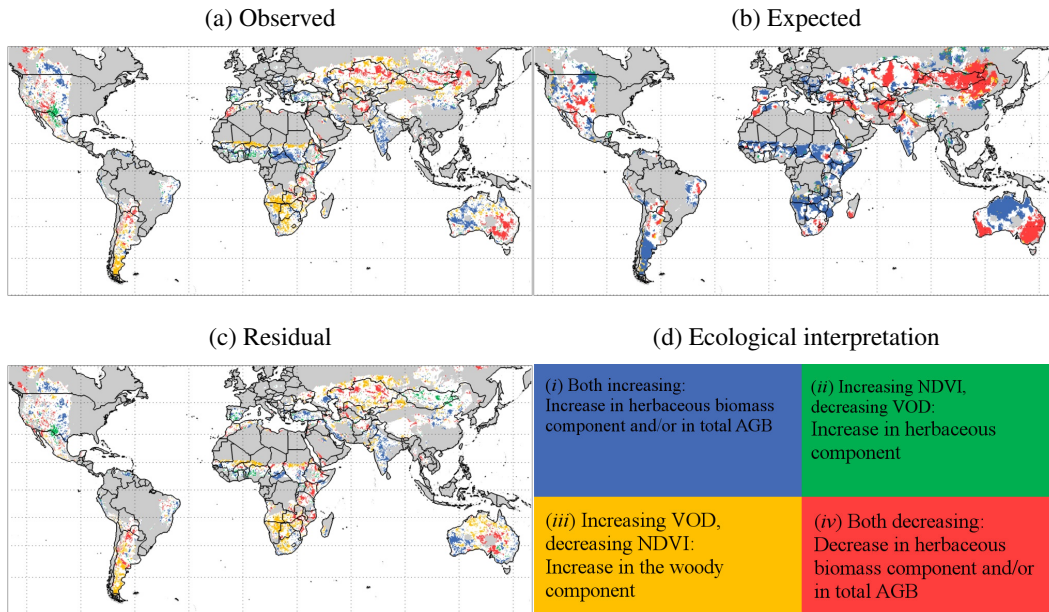


**Fig. 11.** Co-relationship of NDVI and VOD trends stratified into four classes: (i) both increasing; (ii) increasing NDVI and decreasing VOD; (iii) increasing VOD and decreasing NDVI; and (iv) both decreasing. **(a)** Is the observed trends, **(b)** the expected trends, and **(c)** the residual trends. Only grid cells with significant trends ( $p < 0.05$ ) and less than 60 % missing values in both products are shown. **(d)** Shows the ecological interpretation, based on the four expectations of the background theory section.

Title Page

Abstract

Introduction

Conclusions

References

Tables

Figures

◀

▶

◀

▶

Back

Close

Full Screen / Esc

Printer-friendly Version

Interactive Discussion



Global changes in  
dryland vegetation  
dynamics

N. Andela et al.

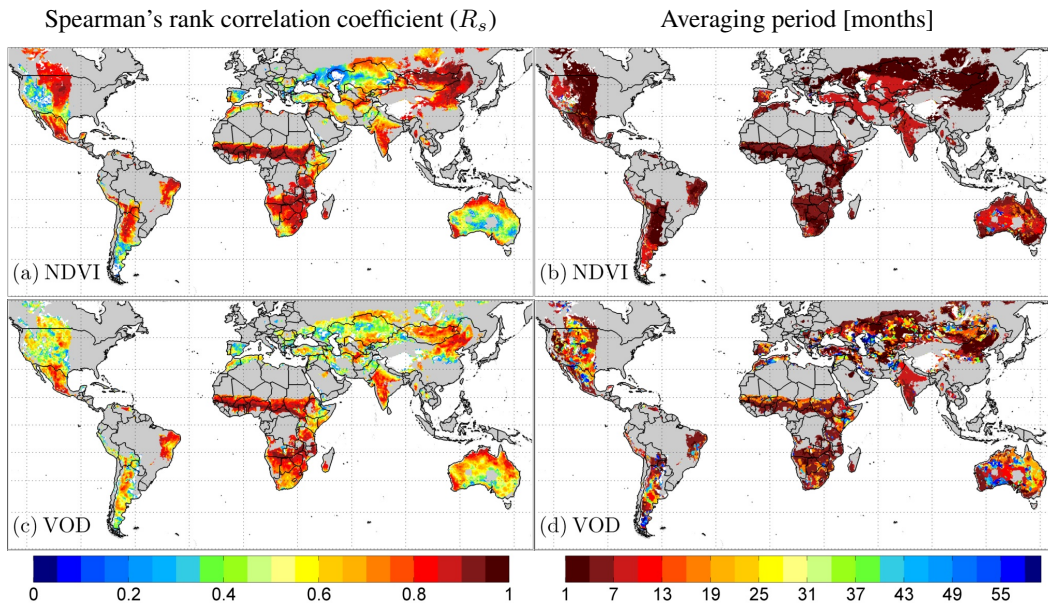


**Fig. A1.** Spearman's rank correlation coefficient ( $R_s$ ) and averaging periods for the two vegetation indices. For the NDVI **(a)** is the  $R_s$  between API and the NDVI and **(b)** is the averaging period for antecedent precipitation that leads to the highest  $R_s$  between PRM and the NDVI, **(c)** and **(d)** are as **(a)** and **(b)** except for the VOD. Grid cells without significant correlation ( $p > 0.05$ ), with over 60 % missing values, or with a negative correlation coefficients are masked (white).

Title Page

Abstract

Introduction

Conclusions

References

Tables

Figures

◀

▶

◀

▶

Back

Close

Full Screen / Esc

Printer-friendly Version

Interactive Discussion

